Core-top calibration of the lipid-based $U^{K'}_{37}$ and TEX_{86} temperature proxies on the southern Italian shelf (SW Adriatic Sea, Gulf of Taranto)

Arne Leider[a, *], Kai-Uwe Hinrichs[a], Gesine Mollenhauer[a, b] and Gerard J.M. Versteegh[a]

[a] *MARUM Center for Marine Environmental Sciences & Dept. of Geosciences, University of Bremen, D-28334 Bremen, Germany*

[b] *Alfred Wegener Institute for Polar and Marine Research, D-27570 Bremerhaven, Germany*

[*] corresponding authors,

E-mail addresses: AL: arneleider@uni-bremen.de; GJMV: versteegh@uni-bremen.de

Phone: +49 421 218 65742 (AL)

Fax: +49 421 218 65715

Abstract

The Mediterranean Sea is at the transition between temperate and tropical air masses and as such of importance for studying climate change. The Gulf of Taranto and adjacent SW Adriatic Sea are at the heart of this region. Their sediments are excellently suited for generating high quality environmental records for the last millennia with a sub-decadal resolution. The quality of these records is dependent on a careful calibration of the transfer functions used to translate the sedimentary lipid signals to the local environment. Here, we examine and calibrate the $U^{K'}_{37}$ and TEX_{86} lipid-based temperature proxies in 48 surface sediments and relate these to ambient sea surface temperatures and other environmental data. The $U^{K'}_{37}$ -based temperatures in surface sediments reflect winter/spring sea surface

temperatures in agreement with other studies demonstrating maximum haptophyte production during the colder season. The TEX_{86} -based temperatures for the nearshore sites also reflect winter sea surface temperatures. However, at the most offshore sites, they correspond to summer sea surface temperatures. Additional lipid and environmental data including the distribution of the BIT index and remote-sensed chlorophyll-*a* suggest a shoreward increase of the impact of seasonal and spatial variability in nutrients and control of planktonic archaeal abundance by primary productivity, particle loading in surface waters and/or overprint by a cold-biased terrestrial TEX_{86} signal. As such the offshore TEX_{86} values seem to reflect a true summer signal to the effect that offshore $U^{K'}_{37}$ and TEX_{86} reconstruct winter and summer temperature, respectively, and hence provide information on the annual temperature amplitude.

Keywords: Mediterranean climate, Southern Adriatic Sea, Gulf of Taranto, SST, surface sediments, $U^{K'}_{37}$, TEX_{86}, BIT, alkenones, GDGTs

1. Introduction

A valid and powerful method to better understand short-term environmental and climate change is to study the past. The interactions between atmosphere and ocean are complex so deciphering them requires quantitative and reliable proxies for key environmental parameters such as temperature, air pressure, sea level and the precipitation-evaporation budget. This is also valid for the Mediterranean climate, which is especially sensitive to climate change due to its location between the subtropical high-pressure belt and mid-latitude westerlies (e.g., Trigo et al., 1999; Xoplaki et al., 2003, 2004).

As Sea Surface Temperature (SST) is an important factor in the Earth's climate, its reconstruction is essential for an understanding of past climate change. The commonly used geochemical temperature proxies include $\delta^{18}O$ and Mg/Ca ratios of planktonic foraminifera (Erez & Luz, 1983; Nürnberg et al., 1996; Elderfield & Ganssen, 2000), the $U^{K'}_{37}$ from alkenones synthesized by haptophytes (Prahl & Wakeham, 1987) and the TEX_{86} based on archaeal isoprenoidal tetraether lipids (Schouten et al., 2002; Kim et al., 2008).

The $U^{K'}_{37}$ exploits the observation that the abundance of the diunsaturated C_{37} methyl alkenone, relative to the total of di- and triunsaturated C_{37} methyl alkenones in surface waters and algal cultures increases with increasing water temperature. These alkenones are produced by a small group of haptophyte algae thriving in the mixed layer: the coccolithophore *Emiliana huxleyi* and related species (Volkman et al., 1980; Marlowe et al., 1984; Brassell et al., 1986; Prahl & Wakeham, 1987; Conte et al., 1998). Global calibrations of marine core-top $U^{K'}_{37}$ values with mean annual SSTs show a consistent linear relationship with an uncertainty of 1.1°C (Müller et al., 1998; Conte et al., 2006). This led to the establishment of the $U^{K'}_{37}$ index as a reliable paleoceanographic tool to estimate SSTs in a variety of oceanic settings (Herbert et al., 2003 and references therein; Haug et al., 2005; Sachs & Anderson, 2005).

Nevertheless, some studies reveal clear discrepancies between the $U^{K'}_{37}$ signal in sediments and annual mean SST (e.g., Volkman, 2000). Factors suggested to cause these discrepancies include preferential degradation of the triunsaturated alkenone (Sun & Wakeham, 1994; Gong & Hollander, 1999; Hoefs et al., 2002; Rontani et al., 2006, 2009; Kim et al., 2009b), influence of nutrients and light (Epstein et al., 1998; Versteegh et al., 2001; Prahl et al., 2003), input of alkenones from remote regions (Benthien & Müller, 2000; Goñi et al., 2001; Ohkouchi et al., 2002; Mollenhauer et al., 2007), differences in species composition (Volkman et al., 1995; Conte et al., 1998), production at greater depths within the euphotic zone (Ternois et al., 1997; Bentaleb et al., 1999; Prahl et al., 2005) or strong blooming of haptophytes in periods with water temperatures that are significantly different from the annual mean (Sikes et al., 1997; Bentaleb et al., 1999; Prahl et al., 2001 and references therein; Popp et al., 2006; Versteegh et al., 2007). In spite of these deviations from the global calibration the utility of site-specific calibrations between environment and $U^{K'}_{37}$ is contentious.

The TEX_{86} temperature proxy is based on archaeal glycerol dialkyl glycerol tetraethers (GDGT), which are abundant in marine sediments (Schouten et al., 2000, 2002). The biological sources are non-hyperthermophilic cren- and euryarchaeota, a major group of prokaryotes in today's oceans and lakes (Karner et al., 2001; Powers et al., 2004). The relative distribution of these isoprenoidal GDGTs varies with growth temperature and (similar to the $U^{K'}_{37}$) linear regressions of core-top TEX_{86} values to SST enable the use of the TEX_{86} as a temperature proxy (Schouten et al., 2002, 2007a; Wuchter et al., 2005; Kim et al., 2008, 2010). The TEX_{86} is considered to reflect annual mean temperatures of the upper mixed layer (Schouten et al., 2002; Kim et al., 2008). Although, the TEX_{86} is increasingly used for reconstructing ancient SSTs, a number of issues remain unresolved (Huguet et al., 2006; Pearson et al., 2007). It appears that the TEX_{86} can be biased due to additional production of GDGTs below the mixed layer (Pearson et al., 2001; Huguet et al., 2007; Lee et al., 2008), by seasonality in crenarchaeotal growth (Schouten et al., 2002; Herfort et al., 2006; Huguet et al., 2006, 2007; Menzel et al., 2006; Wuchter et al., 2006) and by the ecology of planktonic cren- and euryarchaeota due to their presence in different water depths of the ocean and the theoretical possibility of GDGT synthesis by marine euryarchaeota (Wuchter et al., 2005; DeLong, 2006, Turich et al., 2007). Additionally, archaea living in sediments of continental margins and the deep-sea may contribute to the GDGT pool and thus influence the TEX_{86} value (Sorensen & Teske, 2006; Lipp et al., 2008; Shah et al., 2008; Lipp & Hinrichs, 2009).

In coastal settings, fluvial input of terrestrial isoprenoidal GDGTs may bias the TEX_{86} (Herfort et al., 2006). Fortunately, this latter bias can be determined by using the Branched and Isoprenoid Tetraether (BIT) index (Hopmans et al., 2004), a ratio between the abundance of branched GDGTs (presumably derived from anaerobic soil bacteria) and crenarchaeol indicating the relative importance of terrestrial organic matter input (Herfort et al., 2006; Kim et al., 2006, Weijers et al., 2006a; Weijers et al., 2006b).

Diagenetic overprints of the TEX_{86} due to changing redox conditions seem to be less important than for other biomarkers (Sinninghe Damsté et al., 2002a; Schouten et al., 2004; Kim et al., 2009b). However, selective degradation during resuspension, transport and redeposition may be significant in some cases and has to be considered for the reliable application of the TEX_{86} as a SST proxy (Mollenhauer et al., 2007; Kim et al., 2009a). Considering these factors, careful assessment of site-specific relations between $U^{K'}_{37}$ values, TEX_{86} and SST is vital to arrive at reliable SST reconstructions.

At the Gallipoli shelf (Gulf of Taranto, southern Italy) the influence of the mid-latitude westerlies, represented by the seasonal modes of the Northern Atlantic Oscillation (NAO), have a significant effect on the region causing for example maxima in precipitation during winter and arrival of Atlantic storm tracks in southern Italy (e.g., Hurrel and Van Loon, 1997; Xoplaki et al., 2004). Sediments at the shelf are suitable for high resolution environmental reconstruction (e.g., Cini Castagnoli et al., 1999b; Versteegh et al., 2007) (Fig. 1). Shallow-water cores revealed the unique potential for high-resolution down-core studies of the past two centuries based on radiometric dating and tephroanalysis (Cini Castagnoli et al., 1990; Bonino et al., 1993). Furthermore, carbonate contents (Cini Castagnoli et al., 1992a, 1992b), thermoluminescence (Cini Castagnoli et al., 1997) and the stable carbon and oxygen isotope compositions of the planktonic foraminfer *G. ruber* show significant decadal to centennial components, assumed to be related to solar forcing (Cini Castagnoli et al., 1999, 2000, 2002, 2005). An alkenone-based SST reconstruction covering 1305 A.D. to 1979 A.D. proposed that $U^{K'}_{37}$ reflects mainly SST of the cooler part of the year. In the same study an imprint was observed of centennial-scale SST variations consistent with the record of atmospheric $\Delta^{14}C$, a proxy for solar energy variability, suggesting a solar forcing mechanism (Versteegh et al., 2007).

Given the suitability of the Gallipoli region for high-resolution climate reconstruction, we carefully calibrated lipid-derived SST proxies in comparison to the most recent environmental conditions over a broader area covering the Italian shelf within the southern Adriatic Sea and Gulf of Taranto, taking into consideration the preservation, transport and other control mechanisms related to these signals.

2. Study Area

The Adriatic Sea is a narrow semi-enclosed sub-basin of the northeastern Mediterranean Sea which is elongated in NW-SE direction (ca. 200x800 km) (Cattaneo et al., 2003) (Fig. 1). Morphologically its northern part is characterized by shallow and gently sloping shelf (Artegiani et al., 1997a). The southern Adriatic Sea is flanked by a steep slope and narrow shelf, except south of the Gargano Promontory, where the shelf broadens to about 70-80 km and the Strait of Otranto where the Adriatic Sea is separated from the Ionian Sea (Artegiani et al., 1997a; Cattaneo et al., 2003; Zavatarelli & Pinardi, 2003).

The circulation of the Adritatic Sea is known to be cyclonic with seasonal variability (Rizzoli & Bergamasco, 1983; Orlić et al., 1992; Artegiani et al., 1997b; Poulain, 2001). There are three main forcing factors affecting the circulation: a) river run-off causing heat loss and low-salinity water gain; b) atmospheric forcing responsible for dense water formation and seasonal differences in circulation; c) exchange via the Strait of Otranto balancing the water budget by intrusion of warm and salty waters from the Ionian Sea (Artegiani et al., 1997a; Cattaneo et al., 2003; Zavatarelli & Pinardi, 2003; Milligan & Cattaneo, 2007).

The northern Po-river system and Apennine rivers located north of the Gargano Promontory play the major role in freshwater supply for the western Adriatic Sea by contributing more than 70% of the total runoff, whereas in the south-western Adriatic Sea rivers are nearly absent (Raicich, 1996). On a seasonal scale increased river runoff is observed in late autumn and late spring corresponding to precipitation maxima and snow melting (Cattaneo et al., 2003). This creates the coastal buoyancy-driven Western Adriatic Current (WAC) characterized as Adriatic Surface Water (ASW), which is confined to a narrow coastal strip flowing southwards along the Italian eastern margin through the Strait of Otranto into the Gulf of Taranto where it mixes with Ionian Sea water masses. Its intensity and extension can also be tracked by the development of a thermal front showing low temperatures of Adriatic Surface Water trapped in the western Adriatic coast (e.g., Morović et al., 2006).

The southern Adriatic open waters show oligotrophic characteristics comparable to the IS and nutrient supply to the euphotic zone depends strongly on vertical stratification and mixing processes (Viličić et al., 1989). Here, the Western Adriatic Current system plays a crucial role for nutrient supply and drives primary production (PP) of the Adriatic Sea. As a consequence, higher pigment concentrations can be observed in satellite images along the Italian coastal zone (Morović, 2002), the Strait of Otranto, around the Apulian Peninsula into the Gulf of Taranto (e.g. Focardi et al., 2009; Zonneveld et al., 2009). For this region remote-sensing shows a negative correlation between seasonal SSTs to chlorophyll-*a*, whereas SSTs and salinity are positively correlated, indicating that main PP takes place during the colder season and demonstrating the influence of freshwater input and associated heat loss (Zonneveld et al., 2009). Additionally, highest phytoplankton densities in the surface layer of the water column are observed in spring and autumn at the western shelf in the middle Adriatic sub-basin as a consequence of intensified continental water input (Totti et al., 2000). Intrusion of Ionian Surface Water (ISW) is restricted to the eastern coast of the Adriatic Sea, balancing the outflow of Adriatic Surface Water. Advection of nutrient-rich Mediterranean waters into the southern Adriatic Sea is also an important productivity factor (Marasović et al., 1995). Nutrient-rich and high-salinity intermediate waters, with a core at 200 m, form the Levantine Intermediate Water (LIW). The Levantine Intermediate Water invades the southern Adriatic Sea during winter at the western Adriatic shelf, where it mixes with Adriatic Surface Water, affecting the phytoplankton community (Caroppo et al., 2001).

Deep-water formation takes place in the northern Adriatic Sea. Here, Northern Adriatic deep Dense Water (NAdDW) occupies the northern shelf, promoted by surface cooling due to wind outbreaks during winter (e.g. Vilibić et al., 2005). Additionally, Adriatic Deep Water (ADW) is formed in the southern Adriatic Sea basin. The two deep waters spread into the Ionian Sea. In the Gulf of Taranto, where the width of the shelf rapidly decreases, dense coastal water is released to depth and transformed by intrusion and mixing with ambient water (Kourafalou, 2001; Sellschopp & Alvaréz, 2003; Hainbucher et al., 2006; Bignami et al., 2007).

SSTs from satellite and limited available in-situ measurements in the research area vary between 13 °C in winter and 26 °C in summer and show a good agreement (Zavatarelli et al., 1998; Caroppo et al., 1999, 2001; Socal et al., 1999; Boldrin et al., 2002; Zonneveld et al., 2009). Lower SSTs of 13-15 °C during winter and spring are especially observed at the near-coastal locations in the Gulf of Manfredonia due to the influence of the Western Adriatic Current and freshwater input of the adjacent Ofanto river draining into the gulf.

In the region the upper water column is well mixed during winter and spring while a thermocline starts to develop at 50-70 m water depth in March leading to open-ocean stratification during summer. This controls nutrient distribution, which is additionally influenced by river input and resuspension due to vertical mixing during winter. As a result, nutrient concentrations in the surface waters decrease from NW to SE (e.g., Civitarese et al., 1998). This seasonality in nutrients and other water column characteristics affects the phytoplankton community structure (Boldrin et al., 2002; Socal et al., 1999).

3. Material and methods

3.1 Surface sediment samples

The sediments analyzed represent the top 2 cm of multicores from 48 stations obtained from the southern Adriatic Sea, Strait of Otranto, Cape St. Maria di Leuca and Gulf of Taranto. They have been collected during P339 POSEIDON cruise 'CAPPUCCINO' in June 2006 (Fig. 1, Table 1) (Zonneveld et al., 2009). The material was frozen to -20 °C directly upon collection and stayed at this temperature until geochemical processing. ^{210}Pb ages imply high sedimentation rates along the Italian shelf (compilation in Zonneveld et al., 2009). Given the high sedimentation rates and sampling strategy, samples represent a record of very recent sedimentation between 2 and 29 years.

3.2 Lipid Extraction

For GDGT and alkenone analyses, 5-15 g of freeze dried and homogenized sediment were extracted using an accelerated solvent extractor (ASE 200, DIONEX) with a mixture of dichloromethane (DCM):methanol (MeOH) 9:1 (v/v, three cycles of 5 min each) at 100 °C and 7.6×10^6 Pa. Before extraction known amounts of *n*-hexatriacontane, 2-nonadecanone, *n*-nonadecanol and *n*-nonadecanoic acid were added as internal standards. The obtained total lipid extracts (TLE) were combined and dried using a Turbovap LV (Zymark Corp.) at 35 °C under a nitrogen stream. The dried TLEs were re-dissolved in DCM and subdivided into two aliquots for further purification.

3.3 Alkenone analysis and SST assessment

For alkenone analysis alkenoates were removed by base hydrolysis of the TLE fraction following the procedure described by Elvert et al. (2003). The resulting fraction was separated in DCM-soluble asphaltenes and *n*-hexane-soluble maltenes. The maltenes were desulfurized with activated copper powder and separated by solid phase extraction (Supelco LC-NH_2 glass cartridges; 500 mg sorbent). Four fractions of increasing polarity (hydrocarbons, ketones, alcohols, and fatty acids) were obtained by elution with 4 ml *n*-hexane, 6 ml *n*-hexane:DCM 3:1 (v/v), 7 ml DCM:acetone 9:1 (v/v), and 8 ml 2% formic acid in DCM (v/v). The ketone fraction was dissolved in 100 µl *n*-hexane prior to capillary gas chromatography (GC).

Gas chromatography was performed by using a Trace GC Gas Chromatograph (ThermoQuest) equipped with a 30 m DB-5MS fused silica capillary column (0.32 mm ID, 0.25 µm film thickness) and a flame ionization detector (FID), He as carrier gas with a flow rate of 1 ml/min. The GC temperature program for alkenones used was: injection at 60 °C, 1 min isothermal; from 60 °C to 150 °C at 15 °C/min; from 150 °C to 310 °C at 4 °C/min; 28 min isothermal with a total oven run-time of 75 min. Peak identification of di- and tri-unsaturated C_{37} alkenones ($C_{37:2}$ and $C_{37:3}$) was based on retention time and comparison with parallel GC-MS runs. All samples were analyzed in duplicate and quantification was by peak integration and by assuming the same response factor as the internal standard (2-nonadecanone). Concentrations of di- and triunsaturated C_{37} alkenones are given as sum in ng/g dw (dry weight) sediment.

The $U^{K'}_{37}$ was calculated using the definition of Prahl & Wakeham (1987) and converted into SSTs by applying the sediment core top transfer function of Conte et al. (2006). Analytical precision of duplicate runs was better than ±0.007 $U^{K'}_{37}$ units (±0.02 °C).

3.4 GDGT analysis and SST assessment

For GDGT analysis, TLE aliquots were separated by alumina oxide column chromatography (activated Al_2O_3, basic, ~150 mesh, 58 Å, Type 5016A, Sigma Aldrich) into an apolar and polar fraction using *n*-hexane:DCM 9:1 (v/v) and DCM:MeOH 1:1 (v/v), respectively. The polar fraction was dried under a stream of nitrogen, weighed and dissolved ultrasonically in *n*-hexane:isopropanol 99:1 (v/v) with a concentration of 2 mg/ml (Schouten et al., 2009). The polar fraction containing the GDGTs was filtered using a 0.45 µm pore size PTFE filter prior to analysis as described by Hopmans et al. (2000, 2004).

Analyses were performed by high performance liquid chromatography/atmospheric pressure chemical ionization-mass spectrometry (HPLC/APCI-MS) using an Agilent 1200 series HPLC coupled to an HP 6120 MSD equipped with automatic injector and HP Chemstation software. 20 µl aliquots were injected on to an Alltech Prevail Cyano column (2.1x150 mm, 3 µm; Grace) maintained at 30 °C. GDGTs were eluted using the following gradient with solvent A (*n*-hexane) and solvent B (5% isopropanol in *n*-hexane): 80% A:20% B for 5 min, linear gradient to 36% B in 45 min. Flow rate was 0.2 ml/min. After each analysis the column was cleaned by back-flush of *n*-hexane:isopropanol 90:10 (v/v) at 0.2 ml/min for 8 min.

Conditions for APCI-MS were as follows: nebulizer pressure $4.1x10^5$ Pa, vaporizer temperature 450 °C, drying gas (N_2) flow 5 l/min and temperature 350 °C, capillary voltage -4 kV, corona 4 µA. For isoprenoidal and non-isoprenoidal GDGTs peak integration of their $[M+H]^+$ ions (m/z 1302, 1300, 1298, 1296, 1292, 1022, 1036, 1050) detected in selective ion monitoring (SIM) mode was used (dwell time=76 ms) (Schouten et al., 2007a). The TEX_{86} ratio was calculated according to Schouten et al. (2002). For temperature conversion we used the calibration with annual mean SST using marine sediment core tops after Kim et al. (2008). Additionally, we provide GDGT based temperatures using the recently published calibration from Kim et al. (2010) in the supplementary material (S1).

To examine the potential influence of terrestrial archaeal GDGTs we applied the BIT index (Hopmans et al., 2004). Selected samples were analyzed in duplicate and analytical precision was determined by replicate injections of laboratory internal reference material with known TEX_{86} and BIT values. Mean deviation from reference samples was -0.01 TEX_{86} units and mean standard deviation of duplicate samples was ±0.013 (±0.72 °C). Deviation of duplicate BIT values was better than 0.01 units. Concentrations of GDGTs were not determined.

3.5 TOC and Environmental data

Total Organic Carbon (TOC) values of the surface sediments were obtained from parallel multicores taken together with our samples and range between 0.17 and 0.96% (Zonneveld et al., 2009). Seasonal chlorophyll-*a* (Chl-*a*) and SST data were derived from compiled SeaWifs satellite data for 2002-2006 A.D. Data were extracted from the OBPG MODIS-Aqua Monthly Global 9-km database (http://reason.gsfc.nasa.gov/OPS/Giovanni/ocean.aqua.shtml) on a 0.1 °-grid resolution. Seasonal sea surface salinity (SSS) data were retrieved from the MEDATLAS bottle database (http://odv.awi.de/data/ocean/medatlasii.html) spanning the last 20 years on a 0.2 °-grid resolution. Data based on the NOAA World Ocean Data Atlas 2005 on a 0.25 °-grid resolution were used for: summer-SSS (sites GeoB 10714 and GeoB 10715), autumn-SSS (GeoB 10731, 10732 and 10733), winter-SSS (GeoB 10748 and 10749) and mean annual SSTs (MA SST) and annual salinity data. Seasons were defined as follows: Winter: December – February (DJF), Spring: March – May (MAM), Summer: June – August (JJA), Autumn: September – November (SON)) (Zonneveld et al., 2009).

3.6 Correlation analysis, cluster analysis and contour plots

Correlation analysis was performed to interpret the relation between the biomarker and environmental data sets. The software XLStat version 7.5.2© was used to create a cross correlation table giving a Pearson correlation coefficient r, for significant ($p<0.05$) and highly significant correlations ($p<0.0001$). Cluster analysis was performed on abundances of GDGT-0 to GDGT-4' using the software PAST (PAleontological STatistics) version 1.96© (Hammer et al., 2001) using euclidian distances and ward linkage. Contour plots were generated with Ocean Data View (ODV) version 4.3.2© (Schlitzer, 2010) using a DIVA gridding algorithm (25 per mil x/y length-scale).

4. Results

4.1 Alkenone-based temperatures ($SST_{UK'37}$)

The alkenone-based temperatures range from 14.9 to 19.5 °C with lower temperatures at near-coastal sites (Fig. 2b, Table 1). This temperature difference varies between 2 to 4 °C and is largest in transects at the Gargano Promontory sites. At the Strait of Otranto there is no obvious gradient except in the southernmost transect (10744-42; 15.7-17.8 °C). The onshore-offshore gradient also occurs in the eastern part of the Gulf of Taranto. In contrast, temperature differences at the western Gulf of Taranto are not significant (17.5-18.0 °C). The $SST_{UK'37}$ are up to 4 °C lower than the annual average satellite-derived SSTs, and are much closer to the winter/spring SSTs (Fig. 3). Correlation of $SST_{UK'37}$ with seasonal satellite-derived SST is poor with the exception of winter SST (Table 2).

4.2 GDGT-based temperatures (SST_{TEX86})

The GDGT-based temperatures vary between 11.0 and 25.8 °C and similar to the alkenone-based SSTs, tend to increase seawards (Fig. 2c, Table 1). Lowest SST_{TEX86} (11.0 and 19.5 °C) occur at near-coastal shelf sites (water depth: <220 m); intermediate values (17.4-22.9 °C) at the outer shelf and shelf break sites (220-733 m) and highest values (23.6-25.8 °C) at the deep ocean sites (>733 m). In the Gulf of Taranto this temperature difference between coast and open ocean approaches 10°C (15.1-25.8°C). The comparison with satellite-derived SSTs shows that neither SST_{TEX86} at shallow-shelf sites nor at the offshore sites agree with annually averaged SSTs (Fig. 2a). The comparison between SST_{TEX86} and water depth shows that calculated temperatures at shallow sites match winter and spring SSTs, whereas sites with water depths exceeding 500 m resemble autumn and summer values (Fig. 3). This pattern also persists when using the recently proposed calibration from Kim et al. (2010; Fig. S1 and Tab. S1). SST_{TEX86} shows a positive correlation with depth (Table 2). It is anti-correlated to chlorophyll-*a,* whereas no correlation exists with $SST_{UK'37}$ and TOC.

4.3 Alkenone concentrations

Summed concentrations of the di- and triunsaturated C_{37} alkenones range between 10 and 500 ng/g of dry sediment (Fig. 4b). At the Gargano Promontory highest concentrations of 200-280 ng/g of dry sediment are observed offshore with a cross-shelf decrease towards the near-coastal sites. Similar concentrations are reached in the Strait of Otranto. Maximum concentrations of 400-500 ng/g of dry sediment are observed between Cape St. Maria di Leuca and Gulf of Taranto, where they decrease seawards and to hardly detectable levels at the deepest sites. The normalization of concentrations to TOC (not shown) does not significantly change the above described pattern based on dry sediment.

4.4 GDGT distributions and BIT-Index

The relative abundance of isoprenoidal GDGTs within the surface sediments shows the typical distribution of planktonic archaeal GDGTs and is dominated by GDGT-4 (crenarchaeol) accounting for 50-55% and GDGT-0 representing 25-40% of total GDGTs (Fig. A2).

The BIT index varies between 0.02 and 0.29 (Table 1) with highest values at the near-coastal sites of the Gargano Promontory and decreasing seaward (Fig. 5). At the Strait of Otranto and Gulf of Taranto, BIT is generally lower (0.02 and 0.09), whereas a decrease with increasing distance from the coast was not found. BIT is inversely correlated to SST_{TEX86} and salinity, whereas a positive correlation is present between BIT and chlorophyll-*a* (Table 2).

5. Discussion

The alkenone- and GDGT-based temperature proxies and recent environmental data clearly demonstrate that in the studied region there is no simple relationship with the annual SST usually observed elsewhere. Of the several mechanisms affecting the temperature proxies we will discuss those, which seem to be of major importance: seasonality, subsurface water production of GDGTs, benthic vs. pelagic origin of GDGTs, and bias caused by the presence of terrigenous GDGTs.

5.1 Seasonal alkenone production and alkenone preservation

The observation that the $SST_{UK'37}$ are consistently lower than annual mean SST suggests that alkenone production predominantly takes place during the cooler part of the year along the southern Italian shelf.

In the investigated region haptophyte production is dominated by *E. huxleyi* and occurs throughout the whole year with maxima between late autumn and spring based on near-coastal sediment trap stations within the Strait of Otranto and water samples from transects along the southern Adriatic coast (Caroppo et al., 1999; Socal et al., 1999). In the mid Adriatic Sea *E. huxleyi* abundance typically increases in April (Totti et al., 2000). It is also prominent at the Gulf of Manfredonia (Rubino et al., 2009; Balestra et al., 2009). In this region the winter distribution of cold and nutrient-rich Adriatic Surface Water is the main factor promoting phytoplankton growth and controlling the species composition (Socal et al., 1999). Second in importance is the intrusion of nutrient-rich Levantine Intermediate Water by affecting the renewal of water layers during winter turbulence (Caroppo et al., 2001). At the near-coastal stations satellite-derived SSTs for winter and observed $SST_{UK'37}$ are in agreement with each other showing lower temperatures and the influence of Adriatic Surface Water (Fig. 3).

In the Mediterranean Sea highest coccolithophore production and fluxes occur during late winter and spring, with *E. huxleyi* as the ubiquitous species in the eastern Mediterranean Sea with its highest abundance within surface waters (Knappertsbusch, 1993; Ziveri et al., 2000). $SST_{UK'37}$ below mean annual values have been reported from particulate material collected in sediment traps and surface sediments of the Mediterranean basin (Ternois et al., 1997; Emeis et al., 2000). Calculating $SST_{UK'37}$ of surface sediments from the northern Ionian Sea (Emeis et al., 2000) and top cm of a sediment core from the Strait of Otranto (Sangiorgi et al., 2003) using the calibration of Conte et al. (2006) provides 16 °C and 14 °C. This also agrees with winter SSTs and with our $SST_{UK'37}$ range of our nearby samples 10716 (14.9 °C) and 10742 (17.8 °C). We estimated the expected sedimentary alkenone composition as a flux-weighted mean on the basis of seasonal cell abundances of *E. huxleyi* and seasonal SSTs from a sediment trap at the Italian shelf in the Strait of Otranto showing maximum cell abundances in November and February (Socal et al., 1999). The estimates are consistent with the alkenone composition in the surface sediments and show a substantially lower SST compared to annual mean SSTs (Table 3).

Satellite-derived surface pigment concentrations for the years 2002-2006 of the investigated sites show a negative correlation with SSTs also suggesting that the major portion of PP takes place during the colder seasons with systematically higher chlorophyll-*a* concentrations at the near-coastal sites (Table 2; Zonneveld et al., 2009). Additionally, TOC and concentrations of alkenones appear higher at near-coastal stations, suggesting a higher PP for this region (Fig. 4b).

In general, chlorophyll-*a* concentrations in the water column follow phytoplankton density. Typically, low values, implying oligotrophic conditions, occur throughout the year, except during winter along the southern Adriatic coast (Caroppo et al., 2001). During winter, highest chlorophyll-*a* concentrations are found within the near-coastal surface layer. This is consistent with high phytoplankton concentrations promoted by the nutrient-rich surface waters of the

Western Adriatic Current. Additionally, vertical mixing during winter months brings nutrients into the surface waters (Zonneveld et al., 2009). In summer a deep chlorophyll maximum exists, which can result in underestimation of haptophyte production during warmer seasons as surface waters are depleted in nutrients and alkenone producers may concentrate at the nutricline (Knappertsbusch, 1993). However, observations at the Strait of Otranto imply that coccolithophorids thrive within the surface waters even during summer (Boldrin et al., 2002). Further evidence of the influence of near-coastal Adriatic Surface Water can be observed in the seaward increase in satellite-derived SST during winter (e.g., Gulf of Manfredonia) (Fig. 3). This partly may explain the seaward increase of $SST_{UK'37}$. Since, the $SST_{UK'37}$ increase appears to be 2 °C higher than that observed by satellites an additional explanation is needed. However, considering the calibration error of 1.1 °C, this temperature increase is not significant. Selective degradation of tri-usaturated alkenones in well oxygenated bottom waters of the Northern Adriatic deep Dense Water and/or Adriatic Deep Water at the deeper sites could lead to an increase of $SST_{UK'37}$ (e.g. Hoefs et al., 1998; Gong & Hollander, 1999; Kim et al., 2009b). The influence of early diagenetic processes at the deeper sites was also considered as a factor affecting the dinoflagellate cyst associations in the region, but since oxygen penetration depth is not significantly related to the cyst accumulation rates, this mechanism appears to be unlikely (Zonneveld et al., 2009). Therefore, we propose that selective degradation of alkenones plays a minor role. Instead we conclude that the observed alkenone-based SSTs are consistent with the general productivity patterns recording primarily the SST during the colder part of the year when biomass is highest.

5.2 Seasonality in production of planktonic archaea

For the offshore sites, the GDGT-derived temperatures agree best with summer SST. The SST_{TEX86} are 7 °C higher than annual mean SST and 10 °C higher than $SST_{UK'37}$ (Fig. 3). That leads to the hypothesis that, in contrast to the haptophytes, offshore the export of biomarker signals from planktonic archaea predominantly takes place during the warm season. During this season oligotrophic conditions in the open Adriatic and Ionian Sea prevail, which is also reflected by minimum concentrations of chlorophyll-*a* in surface waters (Socal et al., 1999). Consequently, maxima in growth of planktonic archaea occur when PP is at a minimum. Such inverse correlations between archaeal abundance and chlorophyll-*a* have also been observed elsewhere such as in the polar oceans (Murray et al., 1998), the Santa Barbara Channel (Murray et al., 1999) and the North Sea (Wuchter et al., 2005; Herfort et al., 2007). GDGT-based SSTs in eastern Mediterranean Sea sediments also agree with our observation that the offshore 'open-sea' sites reflect summer conditions (Menzel et al.,2006; Castañeda et al., 2010). Thus we propose that also for the offshore sites in our study the SST_{TEX86} reflects summer planktonic archaeal production.

In contrast, the much lower SST_{TEX86}, at the near-coastal sites, which agree with winter SST, suggest that the maximum archaeal production takes place during the colder part of the year; the period with maximum PP. This is especially pronounced at the Gargano Promontory sites under the direct influence of the Western Adriatic Current. Nutrient concentrations and particle loading in the surface waters appear higher during the colder period (Socal et al., 1999). These conditions may favor the presence of planktonic archaea as reported for coastal waters in the Black Sea (Stoica and Herndl, 2007) and the Canadian Arctic (Wells et al., 2006). Wuchter et al. (2005) observed a positive correlation between chlorophyll-*a* and archaeal lipids in surface waters from the Bermuda Atlantic Time-Series (BATS). At the BATS site, wind-induced convective mixing results in nutrient enrichment of surface waters which promotes PP during winter and possibly also growth of planktonic archaea. At the coastal sites in our region, chlorophyll-*a* concentrations are higher than offshore during the whole year (Table 1) and even in summer they exceed offshore winter levels. Consequently, in contrast to the offshore sites, archaeal blooming during the oligotrophic season, as a strategy of minimizing the competition for nutrients (Murray, 1998) is unlikely to occur at the coastal sites. Instead the winter signal may become relatively more important. A crucial process may be the concomitant increased transport of phytoplankton to depth due to aggregation of cells and other suspended matter occurring during higher PP in this coastal shallow setting (Socal et al., 1999). This larger amount of marine snow in combination with a shallow water column would promote an efficient vehicle to carry the GDGTs to the sea floor and primarily export the SST signal during this time of the year (Wuchter et al., 2005; Huguet et al., 2006a, 2007). Further evidence may lie in the biology of planktonic archaea with some members participating in the oxidation of ammonia (Könneke et al., 2005; Wuchter et al., 2006). Especially in shallow and photic estuarine sediments, phytoplankton and microphytobenthos can contribute organic nitrogen (Caffrey et al., 2007). If this nitrogen becomes mineralized to ammonia it supports nitrification by crenarchaeaota (Francis et al., 2005; Nicol & Schleper, 2006).

Alternatively, it is known that crenarchaeota can reside in deeper water (e.g., Karner et al., 2001) and low reconstructed temperatures could result from subsurface production of GDGTs, which seems to play a major role in upwelling areas where TEX_{86} systematically underestimates SSTs (Huguet et al., 2007; Lee et al., 2008). However, as our data show, for stations with depths below the thermocline (> 75 m, i.e., the vast majority of our samples), the observed pattern cannot be explained by invoking a substantial contribution of GDGTs produced below the thermocline. Likewise, deep water production is not relevant for the shallowest, coldest stations (< 75 m) that do not reach below the thermocline.

Our observations suggest that there are two modes of planktonic archaeal growth, which are spatially and temporally separated on the southern Italian shelf. One is consistent with the general observation of preferred oligotrophic conditions accompanied by low PP at the offshore sites. The other mode is directly linked to higher nutrient concentrations at the near-coastal sites, where planktonic archaea are rather associated with particle-rich waters of the Adriatic Surface Water and vertical mixing during the colder season.

Future studies on the seasonal abundances and community structure of planktonic archaea within the water column as well as the distribution of GDGTs for near-coastal and offshore sites are required.

5.3 GDGTs from benthic and pelagic archaeal communities

All samples showed a characteristic marine archaeal GDGT profile, with abundant GDGT-0 and crenarchaeol and lower contributions of GDGT-1 to GDGT-3 and the crenarchaeol regioisomer. Shallow sites show a higher contribution of GDGT-0 than offshore sites and vice versa (Fig. A1). Although crenarchaeol is a predominant marker for planktonic crenarchaeota affiliated with Marine Group 1 (MG1) (Sinninghe Damsté et al., 2002b), it also is biosynthesized by a thermophilic crenarchaeota living in hot springs (Pearson et al., 2004; Zhang et al., 2006; Schouten et al., 2007b; Pitcher et al., 2009). GDGT-0 has been interpreted as a general archaeal core lipid that is synthesized by members distributed throughout the archaeal domain (Koga et al., 1993). In the oceanic water column this compound is probably derived from both planktonic eury- and crenarchaeota. Furthermore, it is likely that cren- and euryarchaeota, including sedimentary affiliates of the MG1 archaea (Inagaki et al., 2006) and other benthic archaea (Teske & Sorensen, 2008) produce similar lipids as their water column relatives (Biddle et al., 2006; Lipp & Hinrichs, 2009). In our region benthic cren- and euryarchaeotal communities were found in sediments located off the Cape of St. Maria di Leuca and bottom waters east off the Gulf of Manfredonia (Yakimov et al., 2006; Martin-Cuadrado et al., 2008), but their influence on the TEX_{86} signal still remains unclear. Turich et al. (2007) differentiated between GDGT abundances in epi- and mesopelagic waters based on a data set of particulate organic matter (POM), where higher abundances of GDGT-0 compared to GDGT-1 to GDGT-4 are observed in epipelagic waters indicating a contribution of group II euryarchaeota. Being aware that studies on POM reflect only snapshots it is striking that we observe a similar pattern in the surface sediments. However, without DNA data, a robust link between the microbial ecology of planktonic archaea and GDGT lipids cannot be established.

5.4 Cold-biased signature from the terrestrial realm

The BIT values in the range of 0.02-0.29 with a seaward decrease are consistent with previously observed values for coastal to open marine environments (Hopmans et al., 2004; Kim et al., 2006). BIT values for coastal marine settings with a high input of OM from rivers are up to 0.98 (Hopmans et al., 2004; Kim et al., 2006). In comparison BIT values of lake sediments from Italy showed a wide range between 0.08 and 0.99 and a highly variable degree of soil OM input (Blaga et al., 2009). Hence, the values at the southern Adriatic Sea and Gulf of Taranto suggest the sediments contain a low contribution of soil OM; implying that the TEX_{86} reflects largely a marine signal. Elevated BIT values occur at locations with higher chlorophyll-*a* concentrations and lower salinity (Table 2), a pattern which is particularly pronounced at the inner shelf of the Gargano Promontory. This indicates an increased supply of terrestrial OM and nutrients, due to the influence of the Western Adriatic Current that stimulates PP. However, the supply of terrestrial GDGTs by nearby local rivers south of the Gargano Promontory (e.g. Ofanto River) cannot be excluded. The generally lower BIT values in the remainder of the southern Adriatic Sea and Gulf of Taranto, even at near-coastal sites, can be related to the absence of river input due to the lack of major rivers on the Apulian Peninsula (Raicich, 1996). It also indicates that the input of land-derived material from the north is low and, more specifically, that the soil-derived fraction of terrestrial OM is low for the region (Walsh et al., 2008). The latter situation is typical for southern Italy since the landscape of the Apulian peninsula is characterized by complex karst landforms. Additionally, variations in autochthonous crenarchaeol production can affect the BIT as observed from discrepancies between BIT and other soil markers (Schmidt et al., 2009). Interestingly, higher BIT values are associated with low SST_{TEX86} predominantly at the

Gargano Promontory area (Table 2). This is in contrast to the general observation that terrestrial isoprenoid GDGTs may alter the TEX_{86} signal leading to an increase of estimated temperature with higher BIT values (Herfort et al., 2006; Weijers et al., 2006). Instead our observations suggest the possibility of an allochthonous, cold TEX_{86} signal that is transported from the continent to shelf sediments. Further investigations on the soils and river sediments in the research area are necessary to reveal their influence on the marine realm.

6. Conclusions

Calibration of the $U^{K'}_{37}$ and TEX_{86} temperature proxies using core-tops along the southern Italian shelf to local SSTs shows that both proxies reflect SSTs that considerably differ from annual mean SSTs. $SST_{UK'37}$ values appear lower than annual mean SSTs. This is attributed to predominant production and export of alkenones during winter and spring fuelled by the Adriatic Surface Water and vertical mixing. SST_{TEX86} increases with distance from shore suggesting that at offshore sites the peak of planktonic archaeal production and the export of related signals take place during summer when conditions are oligotrophic. In contrast, SST_{TEX86} at near-coastal sites is low. This is explained by either one or a combination of the following factors: different timing of archaeal production due to particle-rich surface waters and prevailing higher nutrient contents (no oligotrophic conditions) and/or terrestrial input leading to a cold-biased TEX_{86} signal. Our study demonstrates the importance of constraining regional factors to arrive at a robust interpretation of past temperature signals and that care has to be taken in applications of SST proxies in near-coastal environments. We suggest that regional studies are needed in coastal to marine transitions showing contrasting water column characteristics. As a corollary, interpretation of molecular SST signals in terms of absolute temperature in ancient environments that are not accessible to an evaluation of regional and seasonal factors will remain problematic. Here, a combination of both molecular temperature proxies provides an opportunity to differentiate between seasonal and/or spatial characteristics of the water column in the past.

Acknowledgements

We would like to thank M. Elvert, X. Prieto-Mollar and R. Kreutz for lab assistance, E. Schefuß for providing ASE extraction facility and K. Becker for help with sample preparation. Many thanks go to the members of MOCCHA (Multisdisciplinary study of continental/ocean climate dynamics using high-resolution records from the eastern Mediterranean) for fruitful discussion at early stages of this study. This work was supported by the Deutsche Forschungsgemeinschaft under the EUROCORES Programme EuroMARC project MOCCHA, through contract No. ERAS-CT-2003-980409 of the European Commission, DG Research, FP6. Additional support was provided by the Bremen International Graduate School for Marine Sciences “Global Change in the Marine Realm” (GLOMAR). We thank John Volkman and one anonymous reviewer for their constructive comments helping to improve this manuscript.

References:

Artegiani, A., Paschini, E., Russo, A., Bregant, D., Raicich, F., Pinardi, N., 1997. The Adriatic Sea general circulation. Part I: Air–sea interactions and water mass structure. J. Phys. Oceanogr. 27, 1492-1514.

Artegiani, A., Paschini, E., Russo, A., Bregant, D., Raicich, F., Pinardi, N., 1997b. The Adriatic Sea general circulation. Part II: baroclinic circulation structure. J. Phys. Oceanogr. 27, 1515-1532.

Balestra, B., Marino, M., Monechi, S., Marano, C., Locaiono, F., 2009. Coccolithophore communities in the Gulf of Manfredonia (Southern Adriatic Sea): data from water and surface sediments. Micropaleontology 54, 377-396.

Bentaleb, I., Grimalt, J.O., Vidussi, F., Marty, J.C., Martin, V., Denis, M., Hatté, C., Fontugne, M., 1999. The C_{37} alkenone record of seawater temperature during seasonal thermocline stratification. Mar. Chem. 64, 301-313.

Benthien, A., Müller, P.J., 2000. Anomalously low alkenone temperatures caused by lateral particle and sediment transport in the Malvinas Current region, western Argentine Basin. Deep-Sea Res. I 47, 2369-2393.

Biddle, J.F., Lipp, J.S., Lever, M.A., Lloyd, K.G., Sorensen, K.B., Anderson, R., Fredricks, H.F., Elvert, M., Kelly, T.J., Schrag, D.P., Sogin, M.L., Brenchley, J.E., Teske, A., House, C.H., Hinrichs, K.-U., 2006. Heterotrophic Archaea dominate sedimentary subsurface ecosystems off Peru. Proc. Natl. Acad. Sci. USA 103, 3846-3851.

Bignami, F., Sciarra, R., Carniel, S., Santoleri, R., 2007. Variability of Adriatic Sea coastal turbid waters from SeaWiFS imagery. J. Geophys. Res. 112, C03S10, doi: doi:10.1029/2006JC003518.

Blaga, C., Reichart, G.-J., Heiri, O., Sinninghe Damsté, J.S., 2009. Tetraether membrane lipid distributions in water-column particulate matter and sediments: a study of 47 European lakes along a north–south transect. J. .Paleolimn. 41, 523-540.

Boldrin, A., Miserocchi, S., Rabitti, S., Turchetto, M.M., Balboni, V., Socal, G., 2002. Particulate matter in the southern Adriatic and Ionian Sea: characterisation and downward fluxes. J. Mar. Syst. 33-34, 389-410.

Bonino, G., Cini Castagnoli, G., Callegari, E., Zhu, G.-M., 1993. Radiometric and tephroanalysis dating of recent Ionian Sea cores. Il Nuovo Cimento C, 16, 155-162.

Brassell, S.C., Brereton, R.G., Eglinton, G., Grimalt, J., Liebezeit, G., Marlowe, I.T., Pflaumann, U., Sarnthein, M., 1986. Palaeoclimatic signals recognized by chemometric treatment of molecular stratigraphic data. Org. Geochem. 10, 649-660.

Caffrey, J.M., Bano, N., Kalanetra, K., Hollibaugh, J.T., 2007. Ammonia oxidation and ammonia-oxidizing bacteria and archaea from estuaries with differing histories of hypoxia. ISME J. 1, 660-662.

Caroppo, C., Fiocca, A., Sammarco, P., Magazzu, G., 1999. Seasonal variations of nutrients and phytoplankton in the coastal SW Adriatic Sea (1995–1997). Bot. Mar. 42, 389-400.

Caroppo, C., Congestri, R., Bruno, M., 2001. Dynamics of Dinophysis sensu lato species (Dinophyceae) in a coastal Mediterranean environment (Adriatic Sea). Cont. Shelf Res. 21, 1839-1854.

Castañeda, I.S., Schefuß, E., Pätzold, J., Sinninghe Damsté, J.S., Weldeab, S., Schouten, S., 2010. Millennial-scale sea surface temperature changes in the eastern Mediterranean (Nile River Delta region) over the last 27,000 years. Paleoceanography 25, PA1208.

Cattaneo, A., Correggiari, A., Langone, L., Trincardi, F., 2003. The late-Holocene Gargano subaqueous delta, Adriatic shelf: Sediment pathways and supply fluctuations. Mar. Geol. 193, 61-91.

Cini Castagnoli, G., Bonino, G., Provenzale, A., Serio, M., 1990. On the presence of regular periodicities in the thermoluminescence profile of a recent sea sediment core. Phil. Trans. R. Soc. Lond. 330, 481-486.

Cini Castagnoli, G., Bonino, G., Provenzale, A., Serio, M., Callegari, E., 1992a. The $CaCO_3$ profiles of deep and shallow Mediterranean sea cores as indicators of past solar-terrestrial relationships. Nuovo Cimento Soc. Ital. Fis. C 15, 547-563.

Cini Castagnoli, G., Bonino, G., Serio, G., Sonett, C.P., 1992b. Common spectral features in the 5500-year record of total carbonate in sea sediments and radiocarbon in tree rings. Radiocarbon 34, 798-805.

Cini Castagnoli, G., Bonino, G., Della Monica, P., Taricco, C., 1997. Record of thermoluminescence in sea sediments in the last millennia. Nuovo Cimento Soc. Ital. Fis. C 20, 1-8.

Cini Castagnoli, G., Bernasconi, S.M., Bonino, G., Della Monica, P., Taricco, C., 1999. 700 year record of the 11 year solar cycle by planktonic foraminifera of a shallow water Mediterranean core. Adv. Space Res. 24, 233-236.

Cini Castagnoli, G., Bonino, G., Della Monica, P., Taricco, C., Bernasconi, S.M., 1999b. Solar activity in the last millennium recorded in the $\delta^{18}O$ profile of planktonic foraminifera of a shallow water Ionian Sea core. Sol. Phys. 188, 191-202.

Cini Castagnoli, G., Bonino, G., Taricco, C., Bernasconi, S.M., 2000. The 11 year solar cycle and the modern Increase in the $\delta^{13}C$ of planktonic foraminifera of a shallow water Mediterranean Sea Core (590-1979). In: Proc. 1st Solar & Space Weather Euroconference. 'The solar cycle and terrestrial climate', Solar and space weather. Santa Cruz de Tenerife. Tenerife. Spain., ESA SP-463, 481-484.

Cini Castagnoli, G., Bonino, G., Taricco, C., Bernasconi, S.M., 2002. Solar radiation variability in the last 1400 years recorded in the carbon isotope ratio of a mediterranean sea core. Adv. Space Res. 29, 1989-1994.

Cini Castagnoli, G., Taricco, C., Alessio, S., 2005. Isotopic record in a marine shallow-water core: Imprint of solar centennial cycles in the past 2 millennia. Adv. Space Res. 35, 504-508.

Civitarese, G., Gačić, M., Vetrano, A., Boldrin, A., Bregant, D., Rabitti, S., Souvermezoglou, E., 1998. Biogeochemical fluxes through the Strait of Otranto (Eastern Mediterranean). Cont. Shelf Res. 18, 773-789.

Conte, M.H., Thompson, A., Lesley, D., Harris, R.P., 1998. Genetic and physiological influences on the alkenone/alkenoate versus growth temperature relationship in Emiliania huxleyi and Gephyrocapsa oceanica. Geochim. Cosmochim. Acta 62, 51-68.

Conte, M.H., Sicre, M.-A., Rühlemann, C., Weber, J.C., Schulte, S., Schulz-Bull, D., Blanz, T., 2006. Global temperature calibration of the alkenone unsaturation index ($U^{K'}_{37}$) in surface waters and comparison with surface sediments. Geochem. Geophys. Geosyst. 7, Q02005, doi: 10.1029/2005GC001054.

DeLong, E.F. (2006). Archaeal mysteries of the deep revealed, Proc. Natl. Acad. Sci. USA 103, 6417-6418.

Elderfield, H., Ganssen, G., 2000. Past temperature and $\delta^{18}O$ of surface ocean waters inferred from foraminiferal Mg/Ca ratios. Nature, 405, 442-445.

Elvert, M., Boetius, A., Knittel, K., Jørgensen, B.B., 2003. Characterization of specific membrane fatty acids as chemotaxonomic markers for sulfate-reducing bacteria involved in anaerobic oxidation of methane. Geomicrobiol. J. 20, 403-419.

Emeis, K.-C., Struck, U., Schulz, H.-M., Rosenberg, R., Bernasconi, S.M., Erlenkeuser, H., Sakamoto, T., Martinez-Ruiz, F., 2000. Temperature and salinity variations of Mediterranean Sea surface waters over the last 16,000 years from records of planktonic stable oxygen isotopes and alkenone unsaturation ratios. Palaeogeogr., Palaeoclim., Palaeoecol. 158, 259-280.

Epstein, B.L., D'Hondt, S., Quinn, J.G., Zhang, J., Hargraves, P.E., 1998. An effect of dissolved nutrient concentrations on alkenone-based temperature estimates. Paleoceanography 13, 122-126, PA03358.

Erez, J., Luz, B., 1983. Experimental paleotemperature equation for planktonic foraminifera. Geochim. Cosmochim. Acta 47, 1025-1031.

Focardi, S., Specchiulli, A., Spagnoli, F., Fiesoletti, F., Rossi, C., 2009. A combinated approach to investigate the biochemistry and hydrography of a shallow bay in the South Adriatic Sea: the Gulf of Manfredonia (Italy). Environ. Monit. Assess., 153, 209-220.

Francis, C.A., Roberts, K.J., Beman, J.M., Santoro, A.E., Oakley, B.B., 2005. Ubiquity and diversity of ammonia-oxidizing archaea in water columns and sediments of the ocean. Proc. Natl. Acad. Sci. USA 102, 14683-14688.

Gong, C., Hollander, D.J., 1999. Evidence for differential degradation of alkenones under contrasting bottom water oxygen conditions: implication for paleotemperature reconstruction. Geochim. Cosmochim. Acta 63, 405-411.

Goñi, M.A., Hartz, D.M., Thunell, R.C., Tappa, E., 2001. Oceanographic considerations for the application of the alkenone-based paleotemperature $U^{K'}_{37}$ index in the Gulf of California. Geochim. Cosmochim. Acta 65, 545-557.

Hainbucher, D., Rubino, A., Klein, B., 2006. Water mass characteristics in the deep layers of the western Ionian Basin observed during May 2003. Geophys. Res. Lett., 33, L05608.

Hammer, Ø., Harper, D.A.T., Ryan, P.D., 2001. PAST: Paleontological Statistics Software Package for Education and Data Analysis. Palaeontol. Electr. 4, 9.

Haug, G.H., Ganopolski, A., Sigman, D.M., Rosell-Melé, A., Swann, G.E.A., Tiedemann, R., Jaccard, S.L., Bollmann, J., Maslin, M.A., Leng, M.J., 2005. North Pacific seasonality and the glaciation of North America 2.7 million years ago. Nature 433, 821-825.

Herbert, T.D., Heinrich, D.H., Karl, K.T., 2003. Alkenone Paleotemperature Determinations. In: Treatise on Geochemistry, pp. 391-432. Pergamon, Oxford.

Herfort, L., Schouten, S., Boon, J.P., Sinninghe Damsté, J.S., 2006. Application of the TEX_{86} temperature proxy to the southern North Sea. Org. Geochem. 37, 1715-1726.

Herfort, L., Schouten, S., Abbas, B., Veldhuis, M.J.W., Coolen, M.J.L., Wuchter, C., Boon, J.P., Herndl, G.J., Sinninghe Damsté, J.S., 2007. Variations in spatial and temporal distribution of Archaea in the North Sea in relation to environmental variables. FEMS Microbiol. Ecol. 62, 242-257.

Hoefs, M.J.L., Rijpstra, W.I.C., Sinninghe Damsté, J.S., 2002. The influence of oxic degradation on the sedimentary biomarker record I: evidence from Madeira Abyssal Plain turbidites. Geochim. Cosmochim. Acta 66, 2719-2735.

Hopmans, E.C., Schouten, S., Pancost, R.D., van der Meer, M.T.J., Sinninghe Damsté, J.S., 2000. Analysis of intact tetraether lipids in archaeal cell material and sediments by high performance liquid chromatography/atmospheric pressure chemical ionization mass spectrometry. Rap.Commun. Mass. Spectrom. 14, 585-589.

Hopmans, E.C., Weijers, J.W.H., Schefuß, E., Herfort, L., Sinninghe Damsté, J.S., Schouten, S., 2004. A novel proxy for terrestrial organic matter in sediments based on branched and isoprenoid tetraether lipids. Earth Planet. Sci. Lett. 224, 107-116.

Huguet, C., Kim, J.-H., Sinninghe Damsté, J.S., Schouten, S., 2006. Reconstruction of sea surface temperature variations in the Arabian Sea over the last 23 kyr using organic proxies (TEX_{86} and $U^{K'}_{37}$). Paleoceanography 21, PA3003.

Huguet, C., Schimmelmann, A., Thunell, R., Lourens, L.J., Sinninghe Damsté, J.S., Schouten, S., 2007. A study of the TEX_{86} paleothermometer in the water column and sediments of the Santa Barbara Basin. California. Paleoceanography 22, PA3203.

Hurrell, J.W., Van Loon, H., 1997. Decadal variations in climate associated with the North Atlantic Oscillation. Clim. Change 36, 301-326.

Inagaki, F., Nunoura, T., Nakagawa, S., Teske, A., Lever, M., Lauer, A., Suzuki, M., Takai, K., Delwiche, M., Colwell, F.S., Nealson, K.H., Horikoshi, K., D'Hondt, S., Jorgensen, B.B., 2006. Biogeographical distribution and diversity of microbes in methane hydrate-bearing deep marine sediments on the Pacific Ocean margin. Proc. Natl. Acad. Sci. USA 103, 2815-2820.

Karner, M.B., DeLong, E.F., Karl, D.M., 2001. Archaeal dominance in the mesopelagic zone of the Pacific Ocean. Nature 409, 507-510.

Kim, J.-H., Schouten, S., Buscail, R., Ludwig, W., Bonnin, J., Sinninghe Damsté, J.S., Bourrin, F., 2006. Origin and distribution of terrestrial organic matter in the NW Mediterranean (Gulf of Lions): Exploring the newly developed BIT index. Geochem. Geophys. Geosyst. 7, Q11017, doi: 10.1029/2006GC001306.

Kim, J.-H., Schouten, S., Hopmans, E.C., Donner, B., Sinninghe Damsté, J.S., 2008. Global sediment core-top calibration of the TEX_{86} paleothermometer in the ocean. Geochim. Cosmochim. Acta 72, 1154-1173.

Kim, J.-H., Crosta, X., Michel, E., Schouten, S., Duprat, J., Sinninghe Damsté, J.S., 2009a. Impact of lateral transport on organic proxies in the Southern Ocean. Quat. Res. 71, 246-250.

Kim, J.-H., Huguet, C., Zonneveld, K.A.F., Versteegh, G.J.M., Roeder, W., Sinninghe Damsté, J.S., Schouten, S., 2009b. An experimental field study to test the stability of lipids used for the TEX_{86} and palaeothermometers. Geochim. Cosmochim. Acta 73, 2888-2898.

Kim J.-H., van der Meer, J., Schouten, S., Helmke, P., Willmott, V., Sangiorgi, F., Koç, N., Hopmans, E.C., Sinninghe Damsté, J.S., 2010. New indices and calibrations derived from the distribution of crenarchaeal isoprenoid tetraether lipids: Implications for past sea surface temperature reconstructions. Geochim. Cosmochim. Acta 74, 4639-4654.

Knappertsbusch, M., 1993. Geographic distribution of living and Holocene coccolithophores in the Mediterranean Sea. Mar. Micropaleontol. 21, 219-247.

Koga, Y., Nishihara, M., Morii, H., Akagawa-Matsushita, M., 1993. Ether polar lipids of methanogenic bacteria: structures, comparative aspects, and biosyntheses. Microbiol. Mol. Biol. Rev. 57, 164-182.

Kourafalou, V.H., 2001. River plume development in semi-enclosed Mediterranean regions: North Adriatic Sea and Northwestern Aegean Sea. J. Mar. Syst. 30, 181-205.

Könneke, M., Bernhard, A.E., De la Torre, J.R., Walker, C.B., Waterbury, J.B., Stahl, D.A., 2005. Isolation of an autotrophic ammonia-oxidizing marine archaeon. Nature 437, 543-546.

Lee, K.E., Kim, J.-H., Wilke, I., Helmke, P., Schouten, S., 2008. A study of the alkenone, TEX_{86}, and planktonic foraminifera in the Benguela upwelling system: Implications for past sea surface temperature estimates. Geochem., Geophys., Geosyst. 9, Q10019, doi: 10.1029/2008GC002056.

Lipp, J.S., Hinrichs, K.-U., 2009. Structural diversity and fate of intact polar lipids in marine sediments. Geochim. Cosmochim. Acta 73, 6816-6833.

Lipp, J.S., Morono, Y., Inagaki, F., Hinrichs, K.-U., 2008. Significant contribution of Archaea to extant biomass in marine subsurface sediments. Nature, 454, 991-994.

Manca, B.B., Kovacevic, V., Gačić, M., Viezzoli, D., 2002. Dense water formation in the southern Adriatic Sea and spreading into the Ionian Sea in the period 1997-1999. J. Mar. Syst. 33-34, 133-154.

Marasović, I., Grbec, B., Morović, M., 1995. Long-term production changes in the Adriatic. Netherl. J. Sea Res. 34, 267-273.

Marlowe, I.T., Green, J.C., Neal, A.C., Brassell, S.C., Eglinton, G., Course, P.A., 1984. Long chain(n-C_{37}-C_{39}) alkenones in the Prymnesiophyceae, distribution of alkenones and other lipids and their taxonomic significance. Brit. Phycolog. J. 19, 203-216.

Martin-Cuadrado, A.-B., Rodriguez-Valera, F., Moreira, D., Alba, J.C., Ivars-Martinez, E., Henn, M.R., Talla, E., Lopez-Garcia, P., 2008. Hindsight in the relative abundance, metabolic potential and genome dynamics of uncultivated marine archaea from comparative metagenomic analyses of bathypelagic plankton of different oceanic regions. ISME J. 2, 865-886.

Menzel, D., Hopmans, E.C., Schouten, S., Sinninghe Damsté, J.S., 2006. Membrane tetraether lipids of planktonic Crenarchaeota in Pliocene sapropels of the Eastern Mediterranean Sea. Palaeogeogr., Palaeoclim., Palaeoecol. 239, 1-15.

Milligan, T.G., Cattaneo, A., 2007. Sediment dynamics in the western Adriatic Sea: From transport to stratigraphy. Cont. Shelf Res. 27, 287-295.

Mollenhauer, G., Inthorn, M., Vogt, T., Zabel, M., Sinninghe Damsté, J.S., Eglinton, T.I., 2007. Aging of marine organic matter during cross-shelf lateral transport in the Benguela upwelling system revealed by compound-specific radiocarbon dating. Geochem., Geophys., Geosyst. 8, Q09004, doi:10.1029/2007GC001603.

Morović, M., 2002. Seasonal and interannual variations in pigments in the Adriatic Sea. J. Earth Syst. Sci. 111, 215-225.

Morović, M., Mati, F., Grbec, B., Dadi, V., Ivankovi, D., 2006. South Adriatic phenomena observable through VOS XBT and other ADRICOSM data. Acta Adriat. 47, 33-49.

Müller, P.J., Kirst, G., Ruhland, G., von Storch, I., Rosell-Melé, A., 1998. Calibration of the alkenone paleotemperature index $U^{K'}_{37}$ based on core-tops from the eastern South Atlantic and the global ocean (60°N-60°S). Geochim. Cosmochim. Acta 62, 1757-1772.

Murray, A.E., Preston, C.M., Massana, R., Taylor, L.T., Blakis, A., Wu, K., DeLong, E.F., 1998. Seasonal and spatial variability of bacterial and archaeal assemblages in the coastal waters near Anvers Island, Antarctica. Appl. Environ. Microbiol. 64, 2585-2595.

Murray, A.E., Blakis, A., Massana, R., Strawzewski, S., Passow, U., Alldredge, A., DeLong, E.F., 1999. A time series assessment of planktonic archaeal variability in the Santa Barbara Channel. Aq. Microb. Ecol. 20, 129-145.

Nicol, G.W., Schleper, C., 2006. Ammonia-oxidising Crenarchaeota: important players in the nitrogen cycle? Trends Microbiol., 14, 207-212.

Nürnberg, D., Bijma, J., Hemleben, C., 1996. Assessing the reliability of magnesium in foraminiferal calcite as a proxy for water mass temperatures. Geochim. Cosmochim. Acta 60, 803-814.

Ohkouchi, N., Eglinton, T.I., Keigwin, L.D., Hayes, J.M., 2002. Spatial and temporal offsets between proxy records in a sediment drift. Science 298, 1224-1227.

Orlić, M., Gačić, M., La Violette, P.E., 1992. The currents and circulation of the Adriatic Sea. Oceanolog. Acta 15, 109-124.

Pearson, A., McNichol, A.P., Benitez-Nelson, B.C., Hayes, J.M., Eglinton, T.I., 2001. Origins of lipid biomarkers in Santa Monica Basin surface sediment: a case study using compound-specific $\Delta^{14}C$ analysis. Geochim. Cosmochim. Acta 65, 3123-3137.

Pearson, A., Huang, Z., Ingalls, A.E., Romanek, C.S., Wiegel, J., Freeman, K.H., Smittenberg, R.H., Zhang, C.L., 2004. Nonmarine crenarchaeol in Nevada hot springs. Appl. Environ. Microbiol. 70, 5229.

Pearson, P.N., van Dongen, B.E., Nicholas, C.J., Pancost, R.D., Schouten, S., Singano, J.M., Wade, B.S., 2007. Stable warm tropical climate through the Eocene Epoch. Geology 35, 211-214.

Pitcher, A., Schouten, S., Sinninghe Damsté, J.S., 2009. In situ production of crenarchaeol in two California hot springs. Appl. Environ. Microbiol. 75, 4443-4451.

Popp, B.N., Prahl, F.G., Wallsgrove, R.J., Tanimoto, J., 2006. Seasonal patterns of alkenone production in the subtropical oligotrophic North Pacific. Paleoceanograpy 21, PA1004.

Poulain, P.-M., 2001. Adriatic Sea surface circulation as derived from drifter data between 1990 and 1999. J. Mar. Syst. 29, 3-32.

Powers, L.A., Werne, J.P., Johnson, T.C., Hopmans, E.C., Sinninghe Damsté, J.S., Schouten, S., 2004. Crenarchaeotal membrane lipids in lake sediments: A new paleotemperature proxy for continental paleoclimate reconstruction? Geology 32, 613-616.

Prahl, F.G., Wakeham, S.G., 1987. Calibration of unsaturation patterns in long-chain ketone compositions for palaeotemperature assessment. Nature 330, 367-369.

Prahl, F.G., Pilskaln, C.H., Sparrow, M.A., 2001. Seasonal record for alkenones in sedimentary particles from the Gulf of Maine. Deep-Sea Res. I 48, 515-528.

Prahl, F.G., Wolfe, G.V., Sparrow, M.A., 2003. Physiological impacts on alkenone paleothermometry. Paleoceanography 18, PA1025.

Prahl, F.G., Popp, B.N., Karl, D.M., Sparrow, M.A., 2005. Ecology and biogeochemistry of alkenone production at Station ALOHA. Deep-Sea Res. I 52, 699-719.

Raicich, F., 1996. On the fresh balance of the Adriatic Sea. J. Mar. Syst. 9, 305-319.

Rizzoli, P.M., Bergamasco, A., 1983. The Dynamics of the coastal region of the northern Adriatic Sea. J. Phys. Oceanogr. 13, 1105-1130.

Rontani, J.-F., Marty, J.-C., Miquel, J.-C., Volkman, J.K., 2006. Free radical oxidation (autoxidation) of alkenones and other microalgal lipids in seawater. Org. Geochem. 37, 354-368.

Rontani, J.F., Zabeti, N., Wakeham, S.G., 2009. The fate of marine lipids: Biotic vs. abiotic degradation of particulate sterols and alkenones in the Northwestern Mediterranean Sea. Mar. Chem. 113, 9-18.

Rubino, F., Saracino, O.D., Moscatello, S., Belmonte, G., 2009. An integrated water/sediment approach to study plankton (a case study in the southern Adriatic Sea). J. Mar. Syst. 78, 536-546.

Sachs, J.P., Anderson, R.F., 2005. Increased productivity in the subantarctic ocean during Heinrich events. Nature 434, 1118-1121.

Sangiorgi, F., Capotondi, L., Nebout, N.C., Vigliotti, L., Brinkhuis, H., Giunta, S., Lotter, A.F., Morigi, C., Negri, A., Reichart, G.-J., 2003. Holocene seasonal sea-surface temperature variations in the southern Adriatic Sea inferred from a multiproxy approach. J. Quatern. Sci. 18, 723-732.

Schlitzer, R., 2010. Ocean Data View, http://odw.awi.de (version 4.3.2).

Schmidt, F., Hinrichs, K.-U., Elvert, M., 2010. Sources, transport, and partitioning of organic matter at a highly dynamic continental margin. Mar. Chem. 118, 37-55.

Schouten, S., Hopmans, E.C., Pancost, R.D., Sinninghe Damsté, J.S., 2000. Widespread occurrence of structurally diverse tetraether membrane lipids: evidence for the ubiquitous presence of low-temperature relatives of hyperthermophiles. Proc. Natl. Acad. Sci. USA 97, 14421–14426.

Schouten, S., Hopmans, E.C., Schefuss, E., Sinninghe Damsté, J.S., 2002. Distributional variations in marine crenarchaeotal membrane lipids: a new tool for reconstructing ancient sea water temperatures? Earth Planet. Sci. Lett. 204, 265-274.

Schouten, S., Hopmans, E.C., Sinninghe Damsté, J.S., 2004. The effect of maturity and depositional redox conditions on archaeal tetraether lipid palaeothermometry. Org. Geochem. 35, 567-571.

Schouten, S., Huguet, C., Hopmans, E.C., Kienhuis, M.V.M., Sinninghe Damsté, J.S., 2007a. Analytical methodology for TEX_{86} paleothermometry by High-Performance Liquid Chromatography/Atmospheric Pressure Chemical Ionization-Mass Spectrometry. Anal. Chem. 79, 2940-2944.

Schouten, S., van der Meer, M.T.J., Hopmans, E.C., Rijpstra, W.I.C., Reysenbach, A.-L., Ward, D.M., Sinninghe Damsté, J.S., 2007b. Archaeal and bacterial Glycerol Dialkyl

Glycerol Tetraether Lipids in hot springs of Yellowstone National Park. Appl. Environ. Microbiol. 73, 6181-6191.

Schouten, S., Hopmans, E.C., van der Meer, J., Mets, A., Bard, E., Bianchi, T.S., Diefendorf, A., Escala, M., Freeman, K.H., Furukawa, Y., Huguet, C., Ingalls, A., Ménot-Combes, G., Nederbragt, A.J., Oba, M., Pearson, A., Pearson, E.J., Rosell-Melé, A., Schaeffer, P., Shah, S.R., Shanahan, T.M., Smith, R.W., Smittenberg, R., Talbot, H.M., Uchida, M., Van Mooy, B.A.S., Yamamoto, M., Zhang, Z., Sinninghe Damsté, J.S., 2009. An interlaboratory study of TEX_{86} and BIT analysis using high-performance liquid chromatography-mass spectrometry. Geochem. Geophys. Geosyst. 10, Q03012, doi: 10.1029/2008GC002221.

Sellschopp, J. and Álvarez, A., 2003. Dense low-salinity outflow from the Adriatic Sea under mild (2001) and strong (1999) winter conditions. J. Geophys. Res. 108(C9), 8104, doi: 10.1029/2002JC001562.

Shah, S.R., Mollenhauer, G., Ohkouchi, N., Eglinton, T.I., Pearson, A., 2008. Origins of archaeal tetraether lipids in sediments: Insights from radiocarbon analysis. Geochim. Cosmochim. Acta 72, 4577-4594.

Sikes, E.L., Volkman, J.K., Robertson, L.G., Pichon, J.-J., 1997. Alkenones and alkenes in surface waters and sediments of the Southern Ocean: Implications for paleotemperature estimation in polar regions. Geochim. Cosmochim. Acta 61, 1495-1505.

Sinninghe Damsté, J.S., Rijpstra, W.I.C., Reichart, G.-J., 2002a. The influence of oxic degradation on the sedimentary biomarker record II. Evidence from Arabian Sea sediments. Geochim. Cosmochim. Acta 66, 2737-2754.

Sinninghe Damsté, J.S., Schouten, S., Hopmans, E.C., van Duin, A.C.T., Geenevasen, J.A.J., 2002b. Crenarchaeol: the characteristic core glycerol dibiphytanyl glycerol tetraether membrane lipid of cosmopolitan pelagic crenarchaeota. J. Lipid Res. 43, 1641-1651.

Socal, G., Boldrin, A., Bianchi, F., Civitarese, G., De Lazzari, A., Rabitti, S., Totti, C., Turchetto, M.M., 1999. Nutrient, particulate matter and phytoplankton variability in the photic layer of the Otranto strait. J. Mar. Syst. 20, 381-398.

Sorensen, K.B., Teske, A., 2006. Stratified communities of active archaea in deep marine subsurface sediments. Appl. Environ. Microbiol. 72, 4596-4603.

Stoica, E., Herndl, G.J., 2007. Contribution of Crenarchaeota and Euryarchaeota to the prokaryotic plankton in the coastal northwestern Black Sea. J. Plankton Res. 29, 699-706.

Sun, M.Y., Wakeham, S.G., 1994. Molecular evidence for degradation and preservation of organic matter in the anoxic Black Sea basin. Geochim. Cosmochim Acta 58, 3395-3406.

Ternois, Y., Sicre, M.A., Boireau, A., Conte, M.H., Eglinton, G., 1997. Evaluation of long-chain alkenones as paleo-temperature indicators in the Mediterranean Sea. Deep-Sea Res. I 44, 271-286.

Teske, A., Sorensen, K.B., 2008. Uncultured archaea in deep marine subsurface sediments: have we caught them all? ISME J. 2, 3-18.

Totti, C., Civitarese, G., Acri, F., Barletta, D., Candelari, G., Paschini, E., Solazzi, A., 2000. Seasonal variability of phytoplankton populations in the middle Adriatic sub-basin. J. Plankton Res. 22, 1735-1756.

Trigo, I.F., Davies, T.D., Bigg, G.R., 1999. Objective climatology of cyclones in the Mediterranean region. J. Clim. 12, 1685–1696

Turich, C., Freeman, K.H., Bruns, M.A., Conte, M., Jones, A.D., Wakeham, S.G., 2007. Lipids of marine archaea: Patterns and provenance in the water-column and sediments. Geochim. Cosmochim. Acta 71, 3272-3291.

Uda, I., Sugai, A., Itoh, Y.H., Itoh, T., 2004. Variation in molecular species of core lipids from the order thermoplasmales strains depends on the growth temperature. J. Oleo Sci. 53, 399-404.

Versteegh, G.J.M., Riegman, R., de Leeuw, J.W., Jansen, J.H.F., 2001. $U^{K'}_{37}$ values for Isochrysis galbana as a function of culture temperature, light intensity and nutrient concentrations. Org. Geochem. 32, 785-794.

Versteegh, G.J.M., de Leeuw, J.W., Taricco, C., Romero, A., 2007. Temperature and productivity influences on $U^{K'}_{37}$ and their possible relation to solar forcing of the Mediterranean winter. Geochem., Geophys., Geosyst. 8, Q09005, doi: 10.1029/2006GC001543

Vilibić, I., Supić, N., 2005. Dense water generation on a shelf: the case of the Adriatic Sea. Ocean Dyn. 55, 403-415.

Viličić, D., Vučak, Z., Škrivanić, A., Gržetić, Z., 1989. Phytoplankton blooms in the oligotrophic open south Adriatic waters. Mar. Chem. 28, 89-107.

Volkman, J.K., Eglinton, G., Corner, E.D.S., Forsberg, T.E.V., 1980. Long-chain alkenes and alkenones in the marine coccolithophorid Emiliania huxleyi. Phytochemistry 19, 2619-2622.

Volkman, J.K., Barrerr, S.M., Blackburn, S.I., Sikes, E.L., 1995. Alkenones in Gephyrocapsa oceanica: Implications for studies of paleoclimate. Geochim. Cosmochim Acta 59, 513-520.

Volkman, J.K., 2000. Ecological and environmental factors affecting alkenone distributions in seawater and sediments. Geochem. Geophys. Geosyst. 1, 2000GC000061, doi: 10.1029/2000gc000061.

Walsh, E.M., Ingalls, A.E., Keil, R.G., 2008. Sources and transport of terrestrial organic matter in Vancouver Island fjords and the Vancouver-Washington Margin: A multiproxy approach using $\delta^{13}C_{org}$, lignin phenols, and the ether lipid BIT index. Limnol. Oceanogr. 53, 1054-1063.

Weijers, J.W.H., Schouten, S., Hopmans, E.C., Geenevasen, J., A.J., David, O.R.P., Coleman, J.M., D., P.R., Sinninghe Damsté, J.S., 2006a. Membrane lipids of mesophilic anaerobic bacteria thriving in peats have typical archaeal traits. Environ. Microbiol. 8, 648-657.

Weijers, J.W.H., Schouten, S., Spaargaren, O.C., Sinninghe Damsté, J.S., 2006b. Occurrence and distribution of tetraether membrane lipids in soils: Implications for the use of the TEX_{86} proxy and the BIT index. Org. Geochem. 37, 1680-1693.

Wells, L.E., Cordray, M., Bowerman, S., Miller, L.A., Vincent, W.F., Deming, J.W., 2006. Archaea in Particle-Rich Waters of the Beaufort Shelf and Franklin Bay, Canadian Arctic: Clues to an Allochthonous Origin? Limnol. Oceanogr. 51, 47-59.

Wuchter, C., Schouten, S., Wakeham, S.G., Sinninghe Damsté, J.S., 2005. Temporal and spatial variation in tetraether membrane lipids of marine crenarchaeota in particulate organic matter: Implications for TEX_{86} paleothermometry. Paleoceanography 20, PA3013.

Wuchter, C., Schouten, S., Wakeham, S.G., Sinninghe Damsté, J.S., 2006. Archaeal tetraether membrane lipid fluxes in the northeastern Pacific and the Arabian Sea: Implications for TEX_{86} paleothermometry. Paleoceanography 21, PA4208.

Xoplaki, E., González-Rouco, J.F., Luterbacher, J., Wanner, H., 2003. Mediterranean summer air temperature variability and its connection to the large-scale atmospheric circulation and SSTs. Clim. Dyn. 20, 723-739.

Xoplaki, E., González-Rouco, J.F., Luterbacher, J., Wanner, H., 2004. Wet season Mediterranean precipitation variability: influence of large-scale dynamics and trends. Clim. Dyn. 23, 63-78.

Yakimov, M.M., Cappello, S., Crisafi, E., Tursi, A., Savini, A., Corselli, C., Scarfi, S., Giuliano, L., 2006. Phylogenetic survey of metabolically active microbial communities associated with the deep-sea coral Lophelia pertusa from the Apulian plateau, Central Mediterranean Sea. Deep-Sea Res. I 53, 62-75.

Zavatarelli, M., Pinardi, N., 2003. The Adriatic Sea modelling system: a nested approach. Ann. Geophys. 21, 345-364.

Zavatarelli, M., Raicich, F., Bregant, D., Russo, A., Artegiani, A., 1998. Climatological biogeochemical characteristics of the Adriatic Sea. J. Mar. Syst. 18, 227-263.

Zhang, C.L., Pearson, A., Li, Y.L., Mills, G., Wiegel, J., 2006. Thermophilic temperature optimum for crenarchaeol synthesis and its implication for archaeal evolution. Appl. Environ. Microbiol. 72, 4419.

Ziveri, P., Rutten, A., de Lange, G.J., Thomson, J., Corselli, C., 2000. Present-day coccolith fluxes recorded in central eastern Mediterranean sediment traps and surface sediments. Palaeogeogr., Palaeoclim., Palaeoecol. 158, 175-195.

Zonneveld, K.A.F., Chen, L., Möbius, J., Mahmoud, M.S., 2009. Environmental significance of dinoflagellate cysts from the proximal part of the Po-river discharge plume (off southern Italy, Eastern Mediterranean). J. Sea Res. 62, 189-213.

Caption of Figures

Fig. 1 Map of the Adriatic and Ionian Sea indicating the study area and general circulation pattern (ISW: Ionian Surface Water, ASW: Adriatic Surface Water, LIW: Levantine Intermediate Water, NAdDW: Northern Adriatic Deep Water; ADW: Adriatic Deep Water; redrawn from Artegiani et al., 1997b, Poulain et al., 2001, Vilibić et al., 2004). Right zoom in 3D-map showing the locations of the surface sediment analyzed in this study (GP: Gargano Promontory; G. of Manfredonia: Gulf of Manfredonia; St.ML: Cape Santa Maria di Leuca). Samples were grouped in accordance to their spatial distribution within the southern Adriatic Sea (circles: GP and G. of Manfredonia, triangles: Strait of Otranto) and Gulf of Taranto (diamonds: E Gulf of Taranto, squares: W Gulf of Taranto).

Fig. 2 Contour plots of SST values for surface sediments along the southern Italian shelf: a) satellite-derived annual mean SST (AM SST); b) alkenone-based temperature ($SST_{UK'37}$); c) GDGT-derived temperature (SST_{TEX86}). Dashed lines are water depth contours (250 m and 1000 m).

Fig. 3 Seasonal SST and proxy variations for the surface sediment sample locations versus multicore top depth. Curves indicate annual mean (AM SST; solid) and seasonal (Wi SST, Sp SST, Su SST, Au SST; dashed) satellite derived SST. Seasons are defined as: Wi SST: Dec-Jan-Feb, Sp SST: Mar-Apr-May, Su SST: Jun-Jul-Aug, Au SST: Sep-Oct-Nov. SSTs based on $U^{K'}_{37}$ are indicated by filled symbols and TEX_{86} by open symbols, respectively. Different symbols represent the spatial sample distribution within the research area (Fig. 1; circles: GP and G. of Manfredonia, triangles: Strait of Otranto, diamonds: E Gulf of Taranto and squares: W Gulf of Taranto). Errors of temperature estimate based on the calibration of Conte et al. (2006) and Kim et al. (2008) are 1.1 °C and 1.7 °C.

Fig. 4 Distribution of a) TOC values and b) content of summed di- and triunsaturated alkenones (in µg/g dw) in surface sediments along the southern Italian shelf. Dashed lines are water depth contours (250 m and 1000 m).

Fig. 5 Contour plot of BIT index values in surface sediments along the southern Italian shelf. Dashed lines are water depth contours (250 m and 1000 m).

Caption of Figures in Appendix

Fig. A1 Cluster analysis and bar plot of relative GDGT abundance in the analyzed surface sediment samples. Numbers correspond to samples listed in Table 1.

Caption of Tables

Table 1 Station data and results of alkenones and GDGT analysis for core top sediments

Table 2 Pearson correlation coefficient (r) detected between biomarker and environmental data ($p<0.05$ and **$p<0.0001$**)

Table 3 Comparison of seasonal abundance of *E. huxleyi*, influence on the SST signal by calculated weighted SST and $SST_{UK'37}$ of surface sediments

Caption of supplementary material (electronic annex)

Figure S1 SST estimates resulting from the calibration by Kim et al. (2008; x-axis) vs. SST estimates according to two new calibrations by Kim et al. (2010; y-axis; open and black circles are TEX^{L}_{86} and TEX^{H}_{86}, based respectively) for the dataset from the southern Italian shelf. The solid line gives the 1:1 line between both temperature estimates. The dashed lines give the linear regression based on the dataset

Table S1 Comparison of TEX_{86} indices and derived temperatures based on the calibrations from Kim et al. (2008, 2010)

***Research Highlights**

- SSTs based on $U^{K'}_{37}$ and TEX_{86} disagree with each other
- SST $U^{K'}_{37}$ seem to reflect maximum alkenone production during colder part of the year
- SST TEX_{86} increase with distance to coast (=water depth)
- Spatially and temporally separated modes of crenarchaeotal growth

Figure1

Click here to download high resolution image

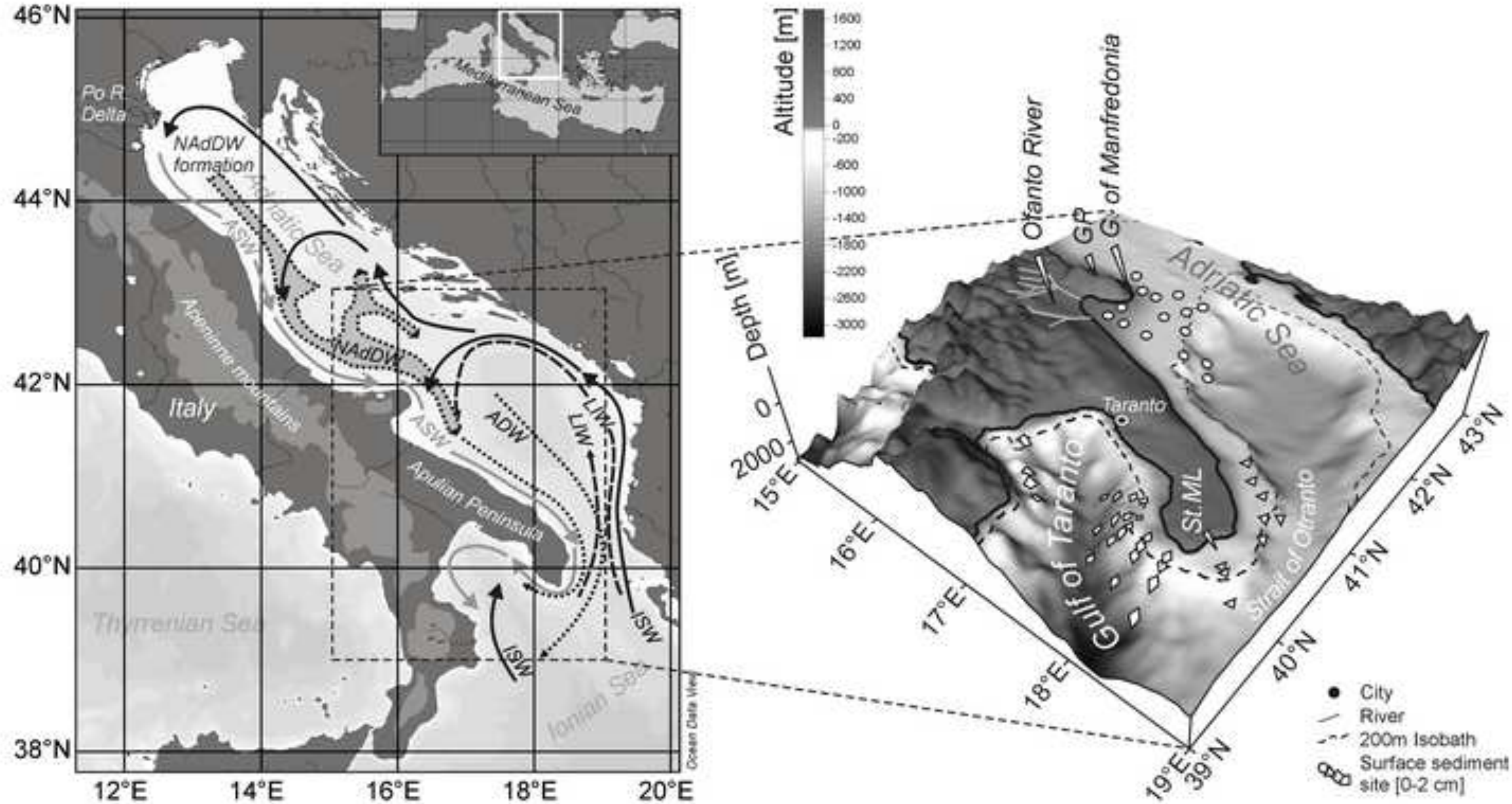

Figure2
Click here to download high resolution image

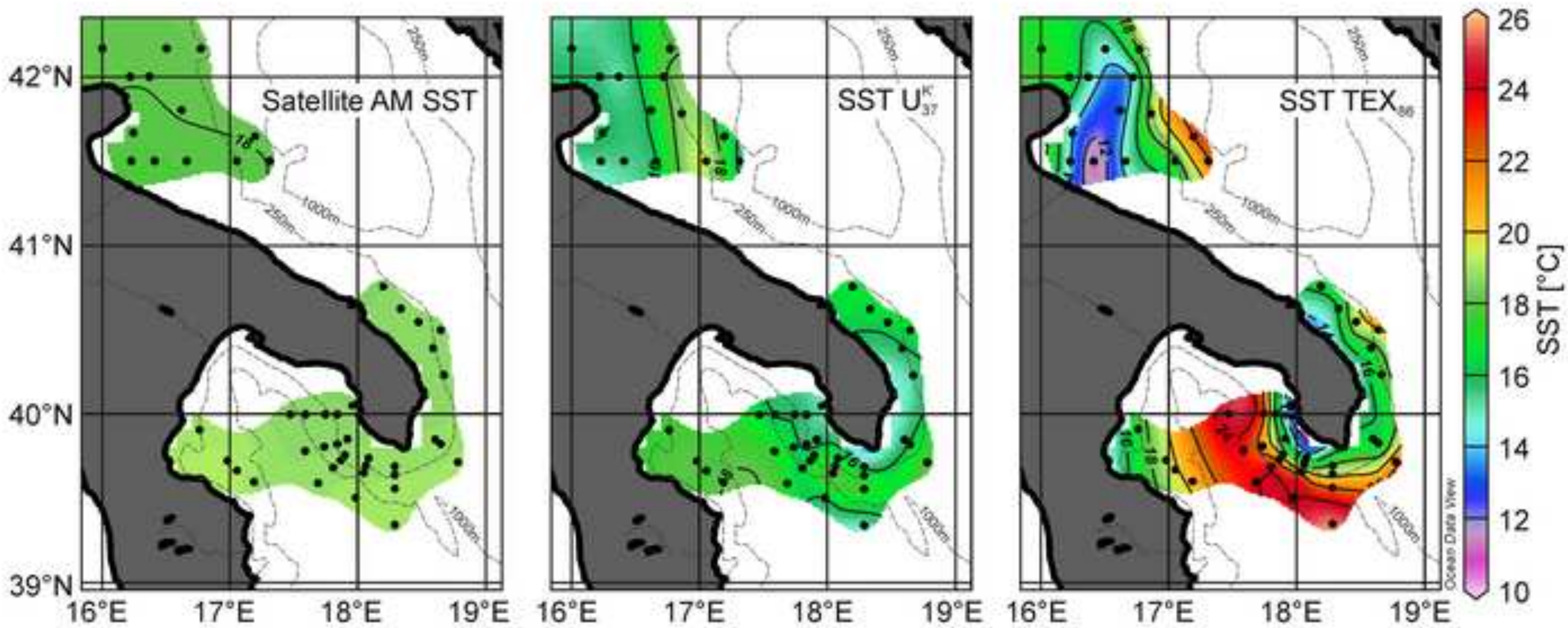

Figure3

Click here to download high resolution image

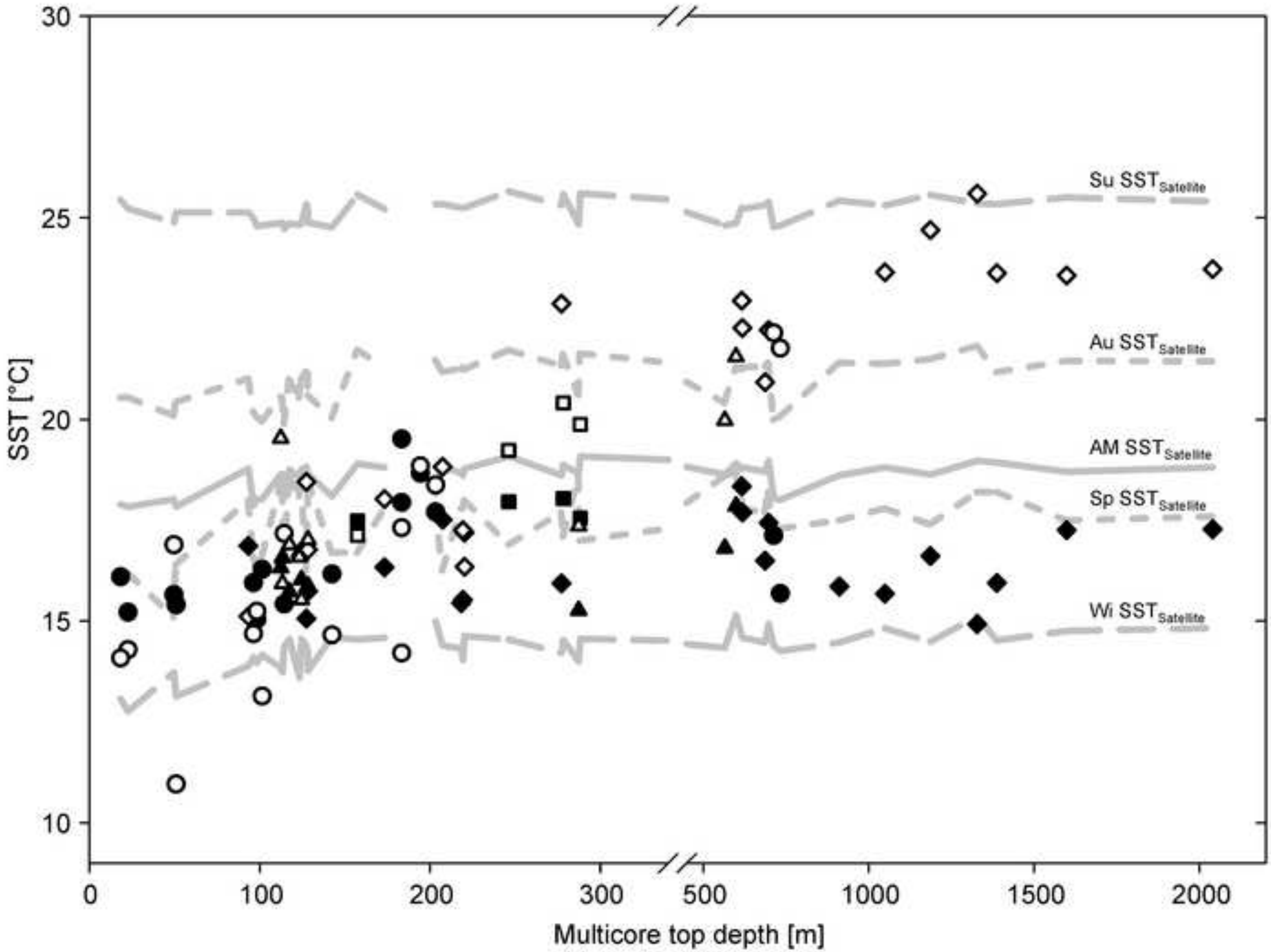

Figure4

Click here to download high resolution image

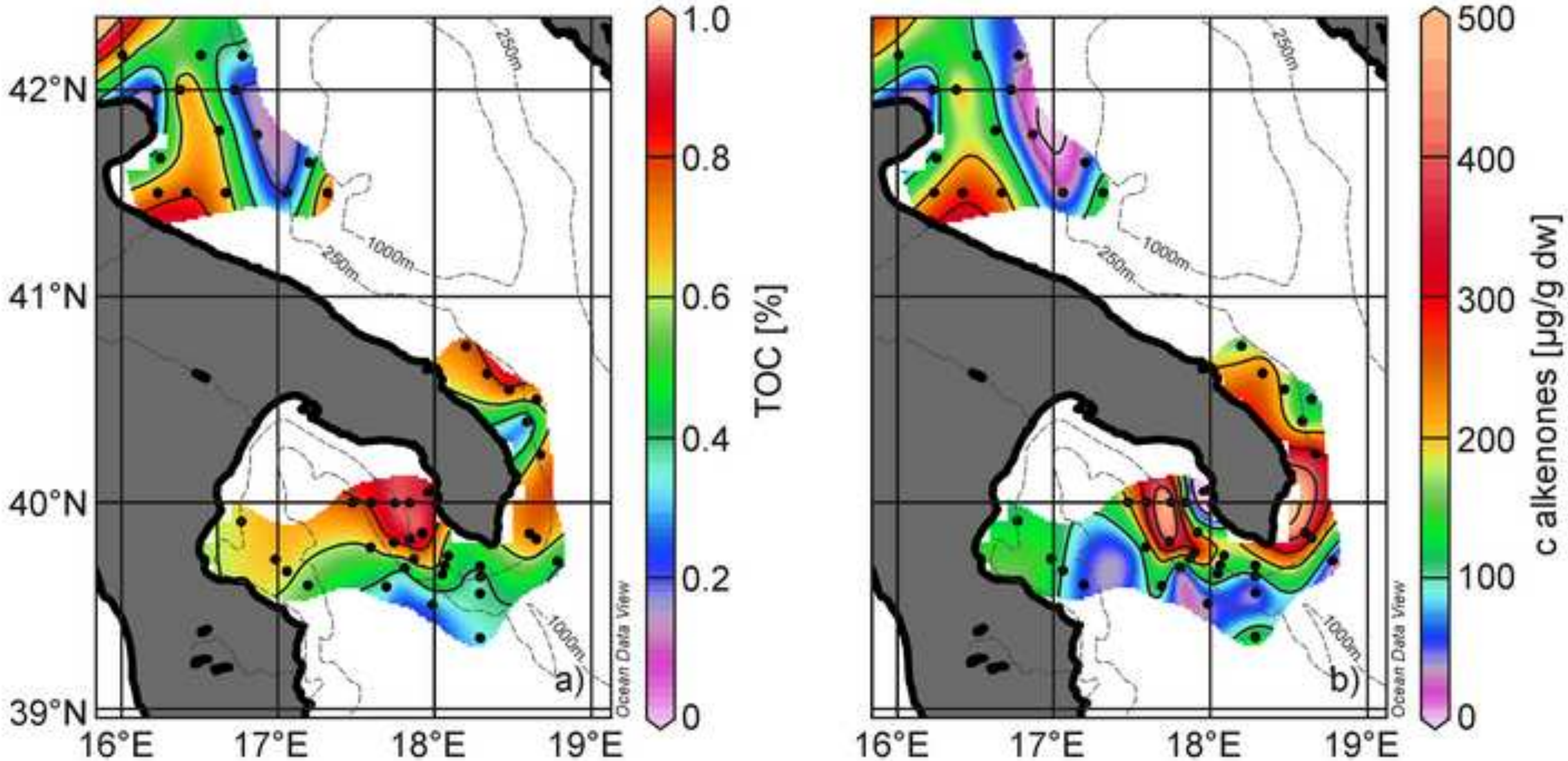

Figure5
Click here to download high resolution image

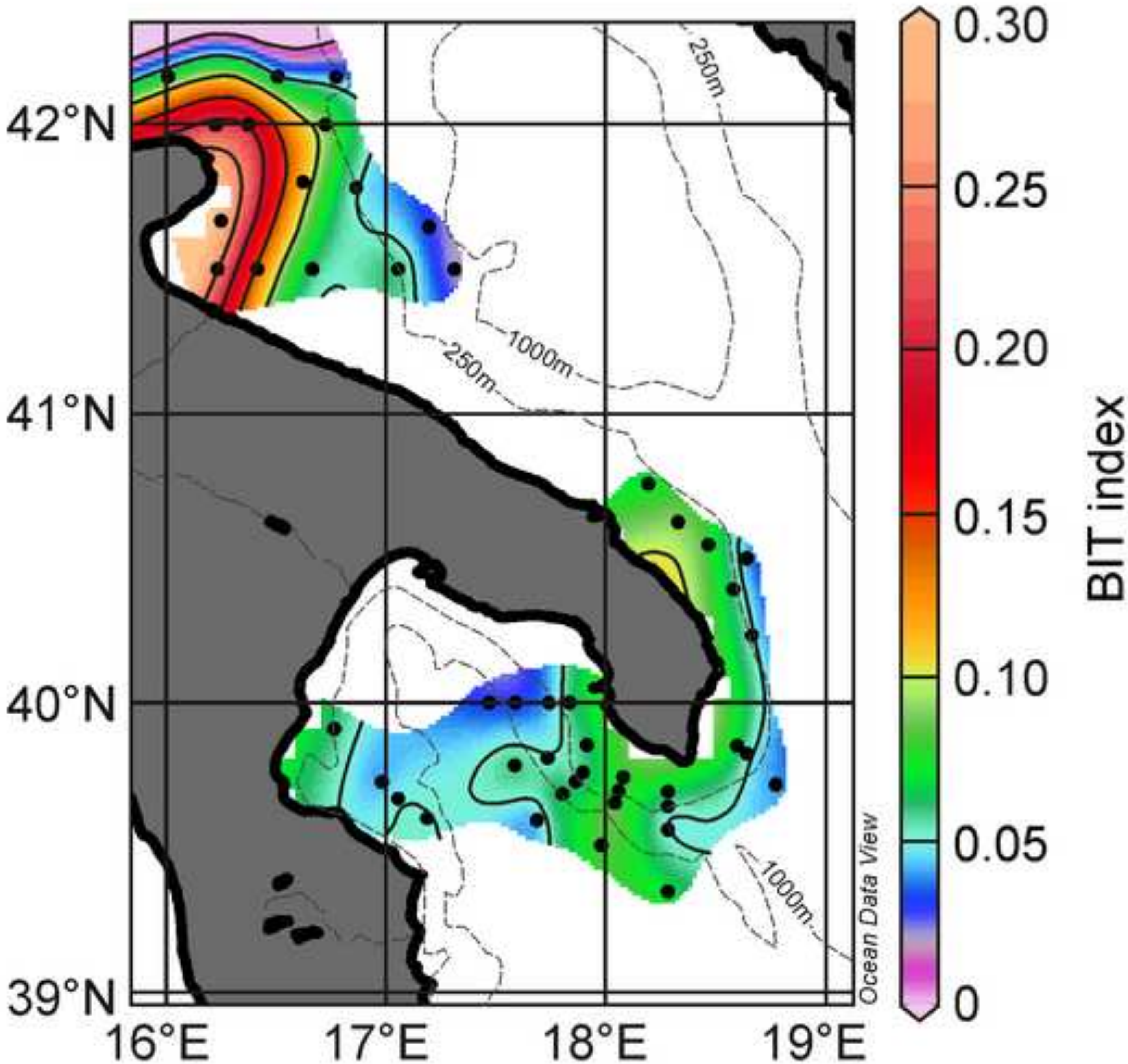

Table1

Click here to download Table: table1.doc

Sample	Lat	Lon	Water Depth	$U^{K'}_{37}$	$SST_{UK'37}$[a]	TEX_{86}	SST_{TEX86}[b]	BIT	Conc alkenones	TOC	SST satellite [°C][c]					Chl*a* [mg/dm^3][c]				SSS [psu][c]				
[GeoB]	[°N]	[°E]	[m]		[°C]		[°C]	index	[µg/g dw]	[%]	an	sp	su	au	wi	sp	su	au	wi	an	sp	su	au	wi
10701	40.000	17.467	1186	0.601	16.61	0.63	24.70	0.03	194	0.79	18.64	17.40	25.57	21.50	14.49	0.30	0.15	0.22	0.26	38.21	38.58	38.43	38.47	37.96
10702	40.000	17.586	911	0.575	15.86	n.d.	n.d.	0.03	311	0.81	18.62	17.50	25.43	21.41	14.47	0.30	0.16	0.24	0.29	38.20	38.54	38.43	38.46	37.94
10703	40.000	17.742	277	0.578	15.93	0.60	22.86	0.04	502	0.96	18.62	17.70	25.32	21.34	14.21	0.35	0.17	0.25	0.34	38.20	38.52	38.31	38.50	38.46
10704	40.000	17.833	219	0.564	15.52	0.50	17.25	0.06	109	0.92	18.61	17.80	25.26	21.30	14.03	0.35	0.18	0.26	0.37	38.18	38.37	38.31	38.54	38.46
10705	39.853	17.913	128	0.572	15.74	0.49	16.76	0.06	175	0.94	18.67	17.90	25.16	21.14	14.19	0.32	0.18	0.27	0.32	38.18	38.36	38.31	38.52	38.35
10706	39.825	17.833	218	0.561	15.44	n.d.	n.d.	n.d.	n.d.	0.88	18.67	17.80	25.25	21.26	14.31	0.31	0.16	0.25	0.28	38.18	38.42	38.31	38.54	38.35
10707	39.783	17.583	1598	0.622	17.26	0.61	23.57	0.06	125	0.59	18.70	17.50	25.50	21.46	14.75	0.29	0.13	0.21	0.24	38.21	38.64	38.36	38.41	38.24
10708	39.808	17.733	686	0.597	16.50	0.56	20.92	0.05	438	0.81	18.70	17.70	25.32	21.33	14.47	0.29	0.15	0.23	0.27	38.21	38.61	38.46	38.55	38.35
10709	39.757	17.893	173	0.591	16.33	0.51	18.03	0.06	396	n.a.	18.81	17.80	25.22	21.30	14.59	0.28	0.15	0.22	0.25	38.23	38.33	38.31	38.51	38.35
10710	39.592	17.683	2040	0.623	17.27	0.61	23.72	0.04	125	0.37	18.81	17.60	25.41	21.44	14.82	0.26	0.12	0.19	0.22	38.23	38.61	38.61	38.59	38.24
10711	39.683	17.800	1049	0.569	15.68	0.61	23.65	0.07	43.9	0.38	18.81	17.80	25.31	21.38	14.82	0.26	0.13	0.20	0.23	38.23	38.55	38.60	38.55	38.37
10712	39.727	17.862	618	0.637	17.69	0.59	22.27	0.05	112	0.71	18.81	17.80	25.22	21.30	14.59	0.28	0.15	0.22	0.25	38.23	38.55	38.60	38.55	38.37
10713	39.692	18.283	127	0.549	15.06	0.52	18.45	0.07	149	0.46	18.83	16.26	25.34	21.18	14.39	0.28	0.16	0.24	0.31	38.24	38.18	37.98	38.31	37.73
10714	39.640	18.283	207	0.631	17.51	0.53	18.83	0.05	82.0	0.33	18.83	16.26	25.34	21.18	14.39	0.28	0.16	0.24	0.31	38.24	38.18	37.98	38.31	37.73
10715	39.559	18.283	697	0.628	17.43	0.59	22.21	0.05	34.4	0.40	18.98	18.20	25.39	21.41	14.92	0.24	0.14	0.18	0.23	38.27	38.30	38.28	38.53	38.12
10716	39.345	18.283	1328	0.544	14.92	0.65	25.60	0.07	133	0.33	18.98	18.20	25.36	21.83	15.11	0.23	0.11	0.15	0.21	38.27	38.38	38.28	38.51	38.34
10717	39.742	18.080	93	0.609	16.86	0.46	15.11	0.08	192	0.45	18.78	18.00	25.14	21.02	13.88	0.33	0.18	0.30	0.39	38.23	38.19	38.31	38.50	38.46
10718	39.693	18.058	220	0.620	17.19	0.48	16.34	0.06	120	0.62	18.78	18.00	25.25	21.24	14.62	0.28	0.15	0.24	0.30	38.23	38.20	38.60	38.52	38.46
10719	39.653	18.042	616	0.658	18.34	0.60	22.95	0.09	143	0.53	18.78	18.00	25.25	21.24	14.62	0.28	0.15	0.24	0.30	38.23	38.27	38.88	38.48	38.72
10720	39.507	17.978	1387	0.578	15.95	0.61	23.63	0.08	38.4	0.28	18.93	18.20	25.34	21.18	14.52	0.26	0.12	0.18	0.23	38.25	38.37	38.88	38.45	38.55
10721	42.166	16.767	203	0.637	17.70	0.52	18.37	0.04	41.6	0.36	18.16	17.90	25.34	21.48	14.99	0.23	0.14	0.20	0.24	38.19	38.36	38.06	38.44	38.44
10722	42.167	16.500	142	0.586	16.17	0.45	14.65	0.05	105	0.45	18.09	16.70	24.76	20.05	14.60	0.25	0.17	0.25	0.28	38.18	38.25	38.11	38.22	38.40
10723	42.167	16.000	114	0.561	15.42	0.50	17.16	0.07	159	0.67	18.06	16.50	24.73	19.90	14.37	0.32	0.23	0.40	0.44	38.10	37.65	37.85	37.88	38.25
10724	42.001	16.217	50	0.568	15.65	0.49	16.89	0.21	54.8	0.21	18.02	15.10	24.89	20.10	13.73	0.40	0.28	0.48	0.70	38.17	37.04	37.86	37.42	37.90
10725	42.000	16.367	98	0.548	15.04	0.46	15.24	0.20	205	0.70	18.02	16.30	24.79	20.06	13.97	0.34	0.24	0.41	0.43	38.17	38.28	37.92	38.15	38.36
10726	42.000	16.717	183	0.645	17.94	0.44	14.20	0.09	40.6	0.21	n.a.	n.a.	n.a.	n.a.	n.a.	n.a.	n.a.	n.a.	n.a.	n.a.	n.a.	n.a.	n.a.	n.a.
10727	41.801	16.617	101	0.589	16.27	0.43	13.14	0.11	122	0.59	18.03	16.60	24.82	19.96	14.16	0.30	0.21	0.32	0.36	38.26	38.02	37.72	38.21	38.47
10728	41.783	16.858	194	0.669	18.66	0.53	18.85	0.05	11.5	0.17	n.a.	n.a.	n.a.	n.a.	n.a.	n.a.	n.a.	n.a.	n.a.	n.a.	n.a.	n.a.	n.a.	n.a.
10729	41.647	17.191	712	0.618	17.12	0.59	22.14	0.03	40.6	0.32	18.05	17.10	24.77	20.00	14.39	0.27	0.13	0.18	0.21	38.27	38.31	38.23	38.48	38.53
10730	41.500	17.050	183	0.698	19.52	0.50	17.30	0.06	24.9	0.21	17.93	17.00	24.66	19.96	14.47	0.26	0.13	0.19	0.22	38.28	38.32	38.10	38.37	38.36
10731	41.500	16.658	96	0.578	15.94	0.45	14.68	0.06	224	0.65	17.87	16.60	25.00	20.19	14.10	0.33	0.26	0.39	0.45	38.27	37.92	37.63	38.07	37.08
10732	41.500	16.407	51	0.560	15.40	0.39	10.96	0.14	283	0.79	17.83	16.40	25.13	20.44	13.14	0.59	0.39	0.58	0.91	38.25	37.60	37.42	38.03	37.08
10733	41.500	16.225	23	0.554	15.22	0.45	14.28	0.25	213	0.73	17.83	16.20	25.23	20.56	12.76	0.79	0.47	0.83	1.43	38.29	37.25	37.31	38.29	37.08
10734	41.667	16.242	18	0.583	16.09	0.44	14.08	0.29	127	0.48	17.89	16.20	25.44	20.54	13.07	1.15	0.67	1.00	1.89	38.29	33.93	37.24	37.59	37.97
10735	41.500	17.308	733	0.569	15.68	0.58	21.77	0.02	129	0.74	18.01	17.30	24.81	20.08	14.25	0.29	0.12	0.18	0.21	38.28	38.58	38.24	38.49	38.59
10736	40.758	18.192	123	0.603	16.69	0.49	16.58	0.07	164	0.76	18.57	18.10	24.82	20.54	13.59	0.36	0.22	0.37	0.54	38.21	38.10	38.00	37.86	37.40
10737	40.625	18.329	113	0.599	16.56	0.48	15.93	0.09	236	0.76	18.64	18.30	24.88	20.56	13.73	0.32	0.20	0.30	0.47	38.18	38.12	37.94	37.93	37.45
10738	40.546	18.467	112	0.591	16.31	0.54	19.54	0.08	189	0.80	18.64	18.40	24.87	20.56	13.84	0.32	0.20	0.31	0.46	38.18	38.28	37.86	37.88	37.45
10739	40.500	18.642	565	0.607	16.80	0.55	19.97	0.04	106	0.66	18.64	18.60	24.82	20.42	14.33	0.26	0.16	0.24	0.30	38.17	38.24	38.09	37.96	37.67
10740	40.392	18.583	128	0.576	15.87	0.49	17.01	0.06	143	0.26	18.66	18.50	24.88	20.60	13.76	0.32	0.19	0.32	0.47	38.16	38.19	38.06	37.79	37.56
10741	40.233	18.667	287	0.556	15.26	0.50	17.35	0.05	330	0.67	18.66	18.60	24.84	20.61	14.00	0.29	0.18	0.29	0.40	37.99	38.18	38.07	37.85	37.64
10742	39.716	18.776	599	0.642	17.85	0.58	21.56	0.04	47.2	0.43	18.91	18.70	24.87	21.30	15.14	0.24	0.14	0.18	0.23	38.26	38.25	37.95	38.37	38.08
10743	39.825	18.642	124	0.581	16.02	0.47	15.52	0.05	271	0.75	18.76	18.60	24.86	21.00	14.55	0.26	0.16	0.21	0.30	38.22	38.10	38.03	38.27	37.66
10744	39.850	18.600	117	0.571	15.72	0.49	16.88	0.07	405	0.72	18.76	18.60	24.86	21.00	14.55	0.26	0.16	0.21	0.30	38.22	38.08	38.02	38.20	37.72
10746	39.908	16.758	157	0.630	17.48	0.50	17.12	0.06	120	0.63	18.90	16.70	25.58	21.73	14.54	0.45	0.21	0.27	0.33	38.26	38.26	38.66	38.38	28.39
10747	39.725	16.975	246	0.646	17.95	0.53	19.23	0.04	134	0.65	19.08	16.90	25.65	21.72	14.54	0.39	0.18	0.24	0.27	38.29	38.27	38.66	38.32	28.39
10748	39.667	17.050	288	0.632	17.55	0.55	19.88	0.05	95.9	0.63	19.08	17.00	25.61	21.64	14.56	0.33	0.16	0.23	0.27	38.29	38.27	38.59	38.29	38.20
10749	39.600	17.183	278	0.648	18.03	0.55	20.41	0.05	55.0	0.54	18.87	17.10	25.59	21.62	14.53	0.32	0.16	0.22	0.26	38.26	38.26	38.66	38.37	38.16

n.d.: not detected

n.a.: not available

[a]$SST_{UK'37}$ calculated after Conte et al., 2006

[b]SST_{TEX86} calculated after Kim et al., 2008

[c]Environmental Data: Chl *a*=Chlorophyll *a*. SSS=Salinity; su=summer (Jun-Jul-Aug), wi=winter (Dec-Jan-Feb) (Zonneveld et al., 2009)

Table2
Click here to download Table: table2.doc

	$SST_{UK'37}$	Conc alkenones	SST_{TEX86}	BIT
Conc alkenones	**-0.415**			
SST_{TEX86}	0.201	-0.145		
BIT	**-0.300**	0.036	**-0.483**	
TOC	**-0.372**	**0.437**	-0.107	-0.065
Water Depth	0.076	-0.134	**<u>0.789</u>**	**-0.317**
SST satellite an	0.237	0.007	**<u>0.532</u>**	**-0.515**
SST satellite sp	0.099	0.157	**0.350**	**<u>-0.537</u>**
SST satellite su	0.192	-0.052	**0.382**	-0.069
SST satellite au	0.234	0.023	**0.522**	**-0.368**
SST satellite wi	**0.381**	-0.222	**<u>0.637</u>**	**<u>-0.695</u>**
Chl *a* sp	-0.191	0.070	**-0.438**	**<u>0.789</u>**
Chl *a* su	-0.271	0.098	**<u>-0.573</u>**	**<u>0.853</u>**
Chl *a* au	**-0.308**	0.097	**<u>-0.570</u>**	**<u>0.878</u>**
Chl *a* wi	-0.275	0.091	**-0.510**	**<u>0.859</u>**
SSS an	**0.331**	-0.269	0.111	0.118
SSS sp	0.166	0.042	**0.448**	**<u>-0.783</u>**
SSS su	**0.382**	-0.144	**<u>0.652</u>**	**<u>-0.609</u>**
SSS au	0.251	-0.046	**0.499**	**<u>-0.545</u>**
SSS wi	-0.183	0.009	0.127	0.014

TOC=Total Organic Carbon; Chl *a*=Chlorophyll *a*; SST=satellite-derived SST; SSS=Salinity; an=annual, sp=spring (Mar-Apr-May), su=summer (Jun-Jul-Aug), au=autumn (Sep-Oct-Nov), wi=winter (Dec-Jan-Feb) (Zonneveld et al., 2009)

Table3

Click here to download Table: table3.doc

	Average occurrence of *E. huxleyi*[a]		SST	SST References
	[cells/dm^{-3}]	[%]	[°C]	
February	22779	47.7	11.2	Socal et al. (1999)
May	8825	18.5	18.8	OBPG MODIS-Aqua 2002-2006*
August	4412	9.2	28.5	Socal et al. (1999)
November	11767	24.6	18.9	OBPG MODIS-Aqua 2002-2006*
MA SST			19.4	
Weighted SST			**16.1**	
$SST_{UK'37}$			**16.2±0.7**	this study (10743 and -44)

[a]Survey from 1994 Socal et al. (1999)

*Monthly means of OBPG MODIS Aqua 2002-2006 for area at Latitude 39.4-39.5 °N/ Longitude 18.3-18.4 °E

Figure A1

Click here to download high resolution image

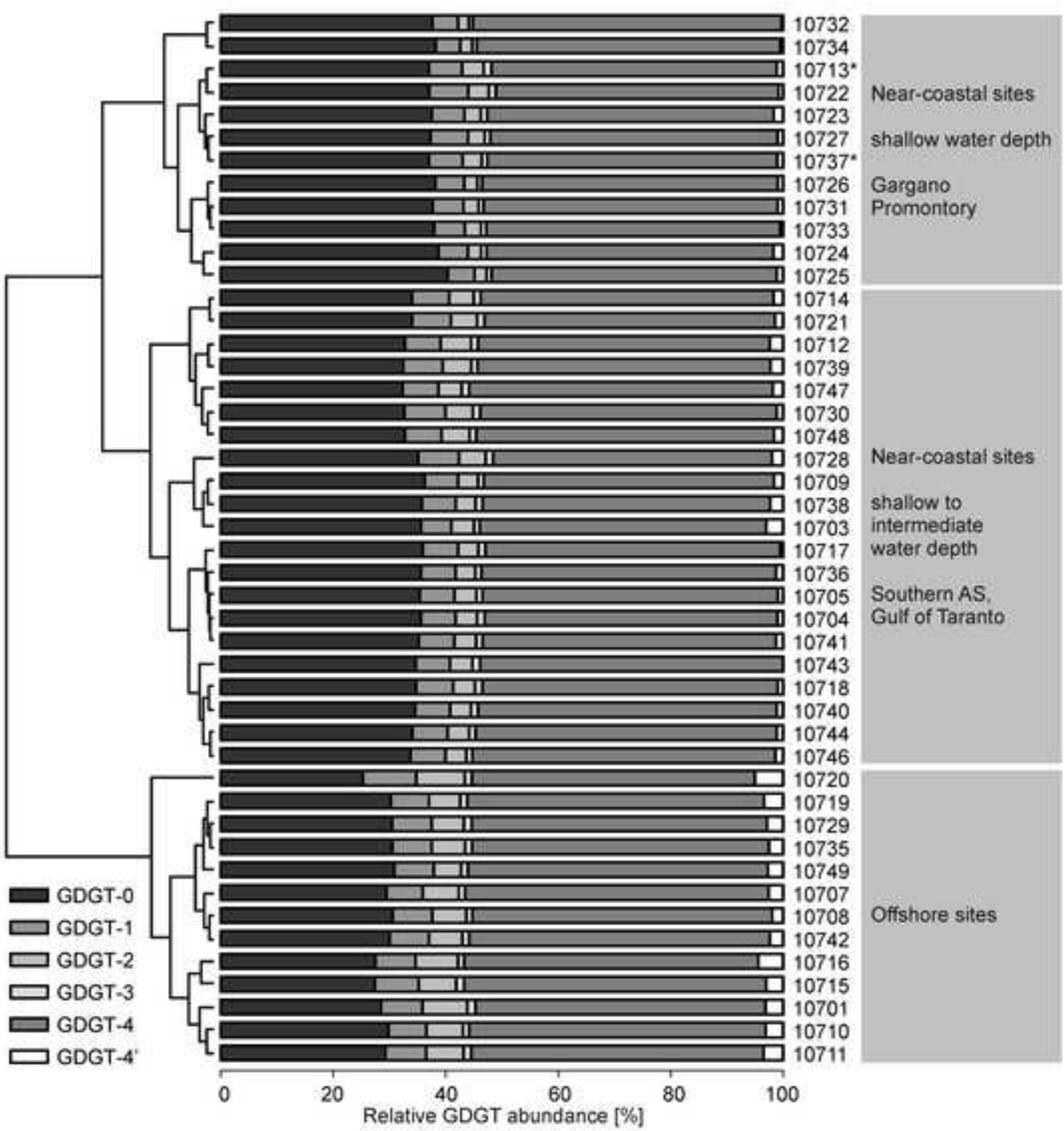

Figure S1

Table S1

Click here to download Supplementary material for on-line publication only: table S1.doc